*Geologie en Mijnbouw* **71**: 259–280, 1993.

# Pressure and temperature history of a low-pressure transitional granulite area, Turku, SW Finland

José A. Van Duin & Carine P. Nieman
*Institute of Earth Sciences, Vrije Universiteit, De Boelelaan 1085, 1081 HV Amsterdam, The Netherlands*

Received 23 October 1991; accepted in revised form 2 December 1992

*Key words:* geothermobarometry, P-T conditions, P-T path, Svecofennian Schist Belt, West Uusimaa granulite Complex

## Abstract

The Turku granulite area forms the westernmost of several low-pressure granulite domains in the Svecofennian Schist Belt of southern Finland. The area shows a gradual transition from amphibolite to granulite facies metamorphism. Estimated peak metamorphic conditions, based on geothermobarometers applied to pelitic gneisses, metavolcanic and charnockitic rocks, are 650–680° C and 4.8 ± 0.5 kbar for the amphibolite domain, 675–725° C and 4.7 ± 0.5 kbar for the transition zone and 750 ± 50° C and 4.9 ± 0.5 kbar for the granulite domain. Prograde and retrograde mineral assemblages of pelitic gneisses indicate a 'clockwise' P-T path.

On the basis of a comparison with other low-P granulite domains occurring in the same belt, namely the West Uusimaa Complex and the Sulkava area, we conclude that all three granulite domains were formed during the same thermal event in the late stage (1850–1800 Ma) of the Svecofennian orogeny. The metamorphic evolution of the Svecofennides is consistent with moderate crustal thickening accompanied by additional heating through thinning of the mantle lithosphere.

## Introduction

Several high-grade granulite terrains occur in two linear zones in Finland parallel to the general strike of the Ladoga Botnian Bay Zone and Svecofennian Schist Belt (Gaál 1982). The Ladoga Botnian Bay Zone crosscuts central Finland in a NNW-SSE direction, and the Svecofennian Schist Belt runs in an E-W direction across southern Finland. From east to west, three granulite facies terrains can be distinguished in this belt (Fig. 1): 1) the Sulkava area, which was extensively studied by Korsman (1977) and Korsman *et al.* (1984); 2) the West Uusimaa granulite Complex northwest of Helsinki (Schreurs 1985a, Schreurs & Westra 1986, Westra & Schreurs 1985, Van Duin 1987); and 3) the Turku granulite area exposed along the southwestern coast of Finland, around Turku (Fig. 2), which was first studied by Hietanen (1947).

Each of these areas shows a gradual transition from the amphibolite to the granulite facies. It is emphasized that the transition to granulite facies does not correspond with a significant depletion in large-ion-lithophile-elements (Kays 1976, Schreurs & Westra 1986).

Radiometric dating in several of these localities indicates ages between 1850 and 1800 Ma for the granulite facies metamorphism. This is consistent with the results obtained from zircons in migmatites from the thermal dome of Sulkava, which produced ages between 1830 and 1810 Ma (Korsman et al. 1984). Monazite and titanite from

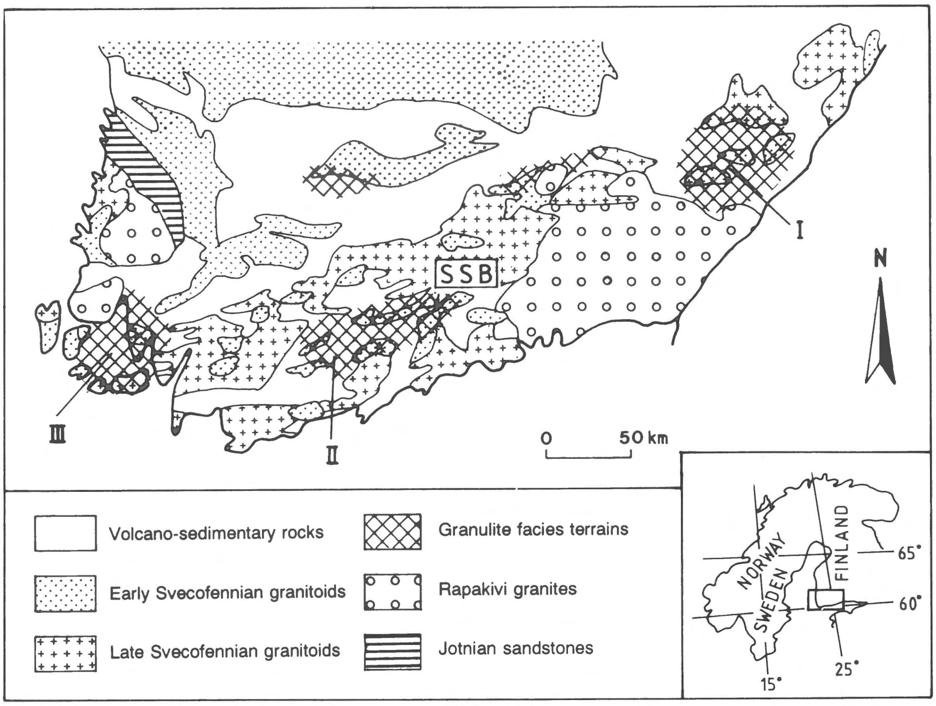

*Fig. 1.* Geological map of southern Finland. Modified after Simonen (1980), Gaál (1982), Huhma (1986) and Front & Nurmi (1987). I-III. LP/HT-granulite facies terrains: I. Sulkava area, II. West Uusimaa granulite Complex, III. Turku granulite area. SSB: Svecofennian Schist Belt.

trondhjemites near Kalanti north of the Turku area yielded U/Pb ages of 1845–1810 Ma, probably related to a thermal event at that time (Patchett & Kouvo 1986).

Thermobarometric studies on supracrustal rocks from different parts of the Turku granulite area (Schellekens 1980, Hangala 1987 (Attu), Hölttä 1986 (Lemu and Mietonen)) all show temperatures in the range 740–800° C and pressures of 4.5–5.5 kbar. Wever (1986) was the first to make a more general study of the high-grade metamorphism of the supra- and infracrustal rocks in the southern part of the Turku granulite domain. His estimates of peak metamorphic conditions range from 700 to 800° C and 4 to 6 kbar, consistent with the earlier reports.

The present study on high-grade rocks from the Turku granulite area was set up as an attempt to document the transition from amphibolite to granulite facies, to create a more detailed and enlarged data set on P-T conditions of the mica gneisses, metavolcanic and charnockitic rocks in the area, and to compare the results with previous studies of the high-grade rocks of southern Finland.

## Geological setting

The Svecofennian Schist Belt consists of a supracrustal sequence of predominantly pelitic gneisses and metavolcanic rocks (1920–1880 Ma; Simonen 1980). This sequence was intruded by early Svecofennian granitoids (1890–1850 Ma) during the main deformation phase (Simonen 1980, Huhma 1986, Patchett & Kouvo 1986). Isoclinal, interfolial folding ($F_1$) was followed by tight folding ($F_2$), which is the dominant deformation phase in the Svecofennides (Ploegsma 1989, Schreurs & Westra 1986). This resulted in a generally steeply dipping E-W to NE-SW trending foliation with transposition of layering and intercalated rock bodies parallel to this

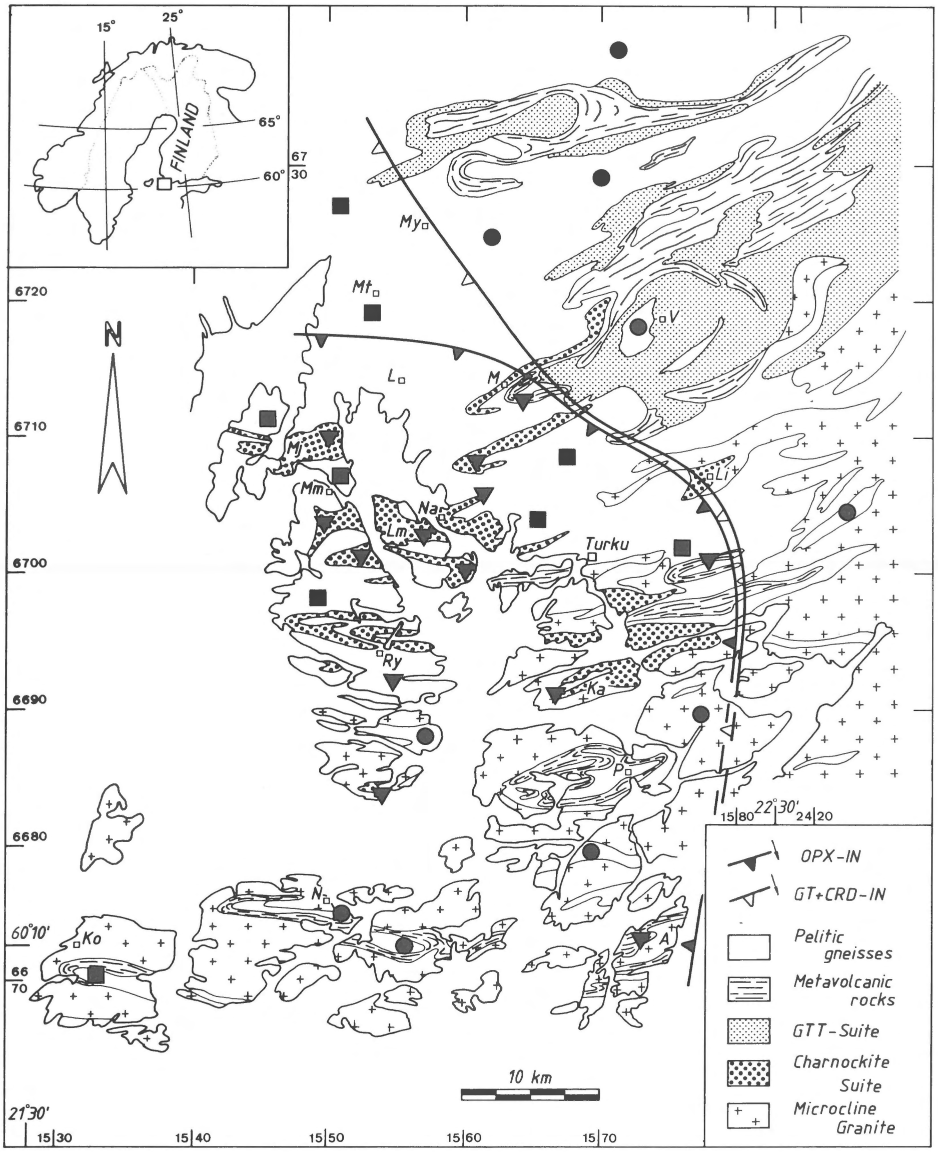

*Fig. 2.* Geological map of the Turku area, compiled from data of Hackman (1923), Hietanen (1947), Härme (1960) and field observations of the authors. Mineral distribution of orthopyroxene (reversed triangles), coexisting garnet + cordierite (squares), and garnet *or* cordierite (circles). The orthopyroxene-IN isograd (OPX-IN) and the garnet-cordierite-IN isograd (GT + CRD-IN) are drawn based on this mineral distribution. GTT-suite: Gabbro/diorite-Tonalite-Trondhjemite suite. *A* = Attu, *Ka* = Kakskerta, *Ko* = Korpo, *L* = Lemu, *Li* = Lieto, *Lm* = Luonnonmaa, *M* = Masku, *Mj* = Merijärvi, *Mm* = Merimasku, *Mt* = Mietonen, *My* = Mynämäki, *N* = Nagu, *Na* = Naantali, *P* = Pargas, *Ry* = Rymättylä, *V* = Vahto.

foliation. Metamorphism to the amphibolite facies occurred at the same time, resulting in migmatization of the metapelitic rocks. Locally, granulite facies conditions were reached. Late Svecofennian granitoids (1850–1880 Ma), which occur exclusively in the Svecofennian Schist Belt, conclude the Svecofennian orogeny in southern Finland (Vaasjoki 1977, Korsman et al. 1984, Front & Nurmi 1987).

The supracrustal rocks exposed in the Turku area are predominantly pelitic garnet- cordierite-mica gneisses, alternated with quartzofeldspathic gneisses, intermediate to mafic metavolcanic rocks and few calc-silicate rocks. The garnet-cordierite-mica gneisses and the quartzofeldspathic gneisses, both highly metamorphosed and migmatized, are of sedimentary origin. They show a compositional banding which corresponds broadly to the original stratification. Occasional preservation of graded bedding has been documented (Hietanen 1947, Härme 1960, Edelman & Jaanus-Järkälä 1984).

*Table 1.* Samples used for geothermobarometry

| Sample no. | Mineral assemblage | Metam. facies |
|---|---|---|
| Pelitic gneisses | | |
| CN151 | Plag-Bio-Qtz-Gt-Preh-Opq-Chl | A |
| CN153 | Gt/Crd-Qtz-Plag-Bio-Kfs-And/Sill-Ilm | A |
| CN133 | Plag-Qtz-Bio-Crd/Gt-Pyr | A |
| CN83 | Crd-Bio-Kfs-Gt-Plag-Qtz-Sill-Pn-Ilm | G |
| CN139 | Plag-Qtz-Bio-Crd-Gt-Kfs-Sill-Ilm-Pyr | G |
| CN143 | Gt-Qtz-Kfs-Plag-Bio-Crd-Sill-Opq-Ilm | G |
| HW166 | Crd-Plag-Qtz-Bio-Gt-Kfs-Sill-Sp | G |
| HW140.6 | Plag-Qtz-Kfs-Gt-Bio-Crd-Pn | G |
| HW138.6 | Plag-Bio-Qtz-Gt-Pn-Gph | G |
| HW143.10 | Qtz-Plag-Bio-Kfs-Gt-Pn-Gph | G |
| CN87b | Plag-Gt-Qtz-Bio-And-Chl-Opq | T |
| CN90 | Plag-Qtz-Kfs-Bio-Gt-Crd-Sill-Pn-Ilm | T |
| Metavolcanic rocks | | |
| HW141.1 | Plag-Opx-Cpx-Bio-Ilm-Pn | G |
| HW013 | Plag-Opx-Bio-Qtz-Cpx-Ilm-Pn | G |
| HW041 | Plag-Opx-Qtz-Ilm-Bio-Gt | G |
| HW043 | Plag-Opx-Hbl-Bio-Cpx-Ilm | G |
| HW137.3 | Plag-Qtz-Opx-Gt-Bio-Ilm-Pn | G |
| HW138.4 | Plag-Qtz-Bio-Opx-Gt-Ilm-Pn | G |
| HW143.6 | Plag-Opx-Qtz-Bio-Cpx-Hbl-Ilm-Pn | G |
| Leuconorites/Hypersthene-bearing tonalites | | |
| HW035 | Plag-Cpx-Bio-Opx-Qtz-Pn | G |
| DU137 | Plag-Opx-Qtz-Bio-Cpx-Pn-Hbl | G |
| DU115 | Plag-Bio-Qtz-Opx-Cpx-Kfs-Pn | G |
| HW147 | Plag-Cpx-Bio-Hbl-Opx-Qtz | G |
| DU72 | Plag-Qtz-Bio-Opx-Cpx-Pn | G |
| DU105 | Plag-Qtz-Bio-Cpx-Opx-Pn | G |
| HW047 | Plag-Cpx-Hbl-Opx-Bio-Ilm-Pn-Qtz | G |

And = andalusite; Bio = biotite; Chl = chlorite; Cpx = clinopyroxene; Crd = cordierite; Gph = graphite; Gt = garnet; Hbl = hornblende; Ilm = ilmenite; Kfs = K-feldspar; Opq = opaque minerals; Opx = orthopyroxene; Plag = plagioclase; Pn =pyrrhotite; Preh = prehnite; Pyr = pyrite; Otz = quartz; Sill = sillimanite; Sp = spinel; A = Amphibolite; T = Transitional; G = Granulite.

The metavolcanic rocks often occur as thin bands interlayered within the metasedimentary gneisses. They locally contain volcanic components like pillow lavas, agglomerates and porphyrites. This supports a volcanosedimentary origin as previously suggested by several authors (Hietanen 1947, Edelman & Jaanus-Järkälä 1984, Ehlers & Lindroos 1986). Marble and calc-silicate rocks form lenses and discontinuous layers within the felsic gneisses and metavolcanic rocks.

Unique for the Turku granulite area is the presence of two early Svecofennian granitoids suites. They are divided into a Gabbro/diorite-Tonalite-Trondhjemite (GTT) suite and a Charnockite suite (Hietanen 1947). The former suite crops out predominantly in the northern part of the area in the amphibolite facies domain, whereas exposure of the Charnockite suite is restricted to the granulite facies domain (Fig. 2). Late Svecofennian garnet-bearing microcline granites are widespread in the area.

### *Amphibolite to granulite transition zone*

The Turku granulite area can be described as a transitional type of granulite domain. In such domains, the boundary between amphibolite facies and granulite facies is commonly drawn at the first occurrence of orthopyroxene in intermediate gneisses. In the pelitic gneisses the prograde transition from amphibolite to granulite facies is located at the first occurrence of coexisting garnet-cordierite mineral pairs, which coincides broadly with the orthopyroxene-IN isograd in intermediate gneisses (Schreurs & Westra, 1986). In the Turku area, we have used the orthopyroxene-IN isograd and also the garnet-cordierite-IN isograd to define the position of the amphibolite- to granulite facies transition (Fig. 2). A suitable orthopyroxene-producing rock type is absent in the northern part of the Turku area and there the boundary of the granulite facies domain is based solely on the garnet-cordierite-IN isograd.

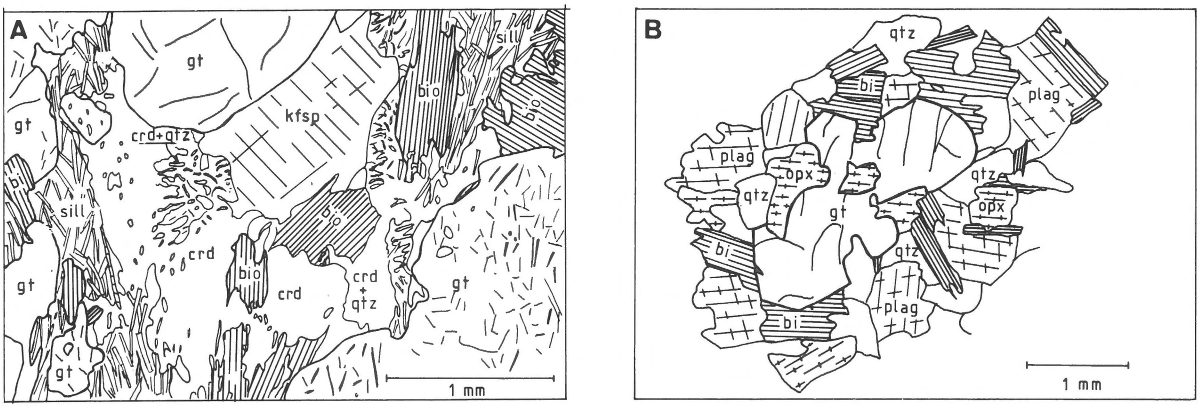

*Fig. 3.* Drawings of mineral textures in pelitic gneisses (A) and intermediate granulite (B). (A) Prograde and retrograde reaction textures involving garnet, cordierite, sillimanite, K-feldspar, biotite and quartz. (B) Garnet overgrowing orthopyroxene. For abbreviations see Table 1.

A suggestion of weak $F_2$-folding of the isograds is present at the eastern granulite boundary between Masku and Lieto. This might indicate that granulite facies metamorphism occurred during the late stages of the main deformation event. $F_2$-folding of the orthopyroxene-IN isograd was also observed in the West Uusimaa granulite Complex (Schreurs 1985a, Schreurs & Westra 1986).

## Petrographic description

This study is based on samples collected by the authors, complemented with samples and data from Wever (1986). Samples, arranged according to rock type, are listed in Table 1.

### *Pelitic gneisses*

The pelitic gneisses consist of banded, strongly foliated and distinctly migmatitic garnet-cordierite-biotite gneisses, alternating with more felsic biotite gneisses. The banding varies from millimetre to centimetre scale, with occasional bands and layers of up to several metres thick. Throughout the area the felsic biotite gneisses contain flattened calc-silicate lenses. The dominant minerals of the pelitic gneisses are quartz, plagioclase, K-feldspar, biotite, garnet and cordierite, with minor quantities of sillimanite and andalusite. Common accessory minerals are zircon, apatite, opaque minerals and tourmaline. In general, garnet-bearing biotite gneisses contain more plagioclase and less K-feldspar than the garnet-cordierite gneisses.

Garnet, cordierite and K-feldspar occur often as porphyroblasts. They may contain inclusions of sillimanite, biotite, quartz and/or plagioclase. Hercynitic spinel included in cordierite was only observed in sample HW85.166 from the core of the granulite domain. Biotite is commonly present as large oriented grains defining the dominant foliation, but it also occurs in symplectites with quartz near cordierite. Symplectitic intergrowths of quartz and cordierite were observed in contact with garnet (Fig. 3A). Small andalusite grains may grow near contacts of cordierite and K-feldspar.

### *Metavolcanic rocks*

The metavolcanic rocks are intermediate to mafic in composition. At the outcrop they show graded bedding and discontinuous banding, and occasionally felsic volcanic bombs. They consist mainly of quartz, plagioclase, K-feldspar, biotite, hornblende and ortho- and/or clinopyroxene. Garnet may be present in minor amounts. Orthopyroxene and clinopyroxene form poikiloblasts with inclusions of quartz, plagioclase, biotite, hornblende and opaques. The poikiloblasts overgrow the biotite foliation. When garnet is present it grows at the expense of orthopyroxene and plagioclase (Fig. 3B). Clinopyroxene has not been observed in garnet-bearing metavolcanic rocks.

### *Charnockite suite*

Rocks belonging to the Charnockite suite occur only within the granulite domain. They vary in composition from gabbro, diorite, leuconorite, quartz diorite, enderbite (orthopyroxene-bearing tonalite) to tonalite. Intrusive bodies of the suite occur as elongated or equidimensional masses concordant to the country rocks. Sills are folded parallel to the regional structure and are strongly foliated, whereas the equidimensional plutons are only weakly foliated along their boundaries. Igneous features like angular mafic enclaves and xenoliths are well preserved.

Coexisting orthopyroxene-clinopyroxene pairs occur only in the leuconorites and enderbites. The dominant minerals in the leuconorites and enderbites are plagioclase, quartz, ortho- and/or clinopyroxene, biotite and hornblende. Plagioclase may exhibit an alignment of phenocrysts in some leuconorites and enderbites. Quartz grains are small and can occur interstitially or as a symplectitic intergrowth with biotite or hornblende. Orthopyroxene and clinopyroxene grew at the expense of biotite and hornblende in the foliated sills, whereas both pyroxenes occur as anhedral to subhedral grains in an equigranular matrix in the plutons. K-feldspar, where present, occurs as interstitial films along grain boundaries and/or as exsolved blebs in plagioclase (antiperthite).

## Mineral chemistry

Minerals used for geothermobarometry have been analysed with a Cambridge Microscan Mark-9 electron microprobe, operating at 20 kV and a sample current of 25 nA. Only fluorine (F) has been measured at 40 nA. The major elements have been calibrated with natural and synthetic standards.

Mineral analyses used for conventional geothermobarometry have been made on cores of five to eight grains for each mineral per sample. Tables 2a, b, 3 and 4a–c give the averages of the mineral compositions for garnet, biotite, cordierite, plagioclase, orthopyroxene and clinopyroxene and include the standard deviation $\sigma_{n-1}$ of $X_{Mg}$ for these averages. Single spot analyses of rims and cores were used for the calculation of P-T conditions with the software package GEO-CALC (Brown et al. 1987, 1988) (Table 6).

### *Garnet*

All garnets are almandine-rich. Those occurring in the matrix are essentially unzoned. In contact with orthopyroxene, cordierite or biotite, the rims (outer 50 to 100 $\mu$m) show a strong Fe-enrichment and a Mg-depletion assumed to be due to (retrogressive) Fe-Mg re-equilibration (Grant & Wieblen 1971). Garnet also shows an enrichment of Mn towards the rim, in agreement with the increase in Mn content with decreasing metamorphic grade (Tracy et al. 1976). Some of the analysed garnets contain some calculated $Fe^{3+}$, up to 2.9% of total Fe.

Garnets coexisting with orthopyroxene in metavolcanics have a relatively high grossular content ($X_{Gr}$ = 0.06–0.13), compared to garnets in mica gneisses ($X_{Gr}$ = 0.02–0.07) (Table 4a).

### *Biotite*

Cores of matrix biotite, isolated from other Fe-Mg phases, were taken to obtain peak metamorphic conditions. A number of grains that have been checked on homogeneity, show that differences between core and rim compositions are insignificant. The biotites are rich in Ti (2.32–4.46 wt%) and F(0.30–1.66 wt%), which is very common for high-grade rocks (Indares & Martignole 1985, Perchuck & Aranovich 1986, Schreurs 1985b). Biotites in contact with garnet or cordierite show higher Mg and often lower Fe (Mg-Fe exchange reaction) and

*Table 2a.* Mineral analyses of orthopyroxene

| | Metavolcanic rocks | | | | Leuconorites/Hypersthene-bearing tonalites | | | | | | |
|---|---|---|---|---|---|---|---|---|---|---|---|
| Ref. | HW | HW | HW | HW | HW | DU | DU | HW | DU | DU | HW |
| No. | 141.1 | 013 | 043 | 143.6 | 035 | 137 | 115 | 147 | 72 | 105 | 047 |
| $SiO_2$ *(wt%)* | 52.22 | 51.62 | 53.94 | 51.12 | 51.31 | 51.60 | 52.42 | 51.41 | 50.17 | 51.87 | 50.44 |
| $Al_2O_3$ | 0.60 | 0.56 | 0.83 | 0.50 | 0.54 | 0.56 | 0.51 | 0.38 | 0.34 | 0.53 | 0.70 |
| $TiO_2$ | 0.09 | 0.14 | 0.13 | 0.04 | 0.06 | 0.08 | 0.06 | 0.07 | 0.09 | 0.08 | 0.05 |
| FeO | 25.49 | 28.11 | 19.34 | 30.97 | 29.81 | 27.53 | 27.09 | 29.35 | 35.27 | 27.81 | 32.16 |
| MnO | 0.84 | 0.55 | 0.56 | 0.79 | 0.54 | 0.50 | 0.87 | 0.83 | 0.93 | 0.84 | 0.66 |
| MgO | 19.92 | 17.74 | 25.04 | 15.59 | 17.06 | 18.49 | 18.94 | 17.35 | 12.52 | 18.11 | 15.42 |
| CaO | 0.72 | 0.80 | 0.63 | 0.74 | 0.76 | 0.74 | 0.57 | 0.89 | 0.85 | 0.71 | 0.81 |
| $Na_2O$ | 0 | 0.02 | 0.05 | 0.02 | 0.01 | 0.02 | 0.01 | 0.02 | 0.03 | 0.02 | 0.04 |
| Total | 99.88 | 99.54 | 100.52 | 99.77 | 100.09 | 99.52 | 100.47 | 100.30 | 100.20 | 99.97 | 100.28 |
| Si *(a.f.u.)* | 1.981 | 1.989 | 1.971 | 1.993 | 1.982 | 1.983 | 1.990 | 1.981 | 1.994 | 1.988 | 1.971 |
| Al | 0.027 | 0.025 | 0.036 | 0.023 | 0.025 | 0.025 | 0.023 | 0.017 | 0.016 | 0.024 | 0.032 |
| Ti | 0.003 | 0.004 | 0.004 | 0.003 | 0.002 | 0.002 | 0.002 | 0.002 | 0.003 | 0.002 | 0.002 |
| Fe | 0.809 | 0.906 | 0.591 | 1.010 | 0.963 | 0.885 | 0.860 | 0.946 | 1.172 | 0.891 | 1.051 |
| Mn | 0.027 | 0.018 | 0.017 | 0.026 | 0.018 | 0.016 | 0.028 | 0.027 | 0.031 | 0.027 | 0.022 |
| Mg | 1.126 | 1.019 | 1.363 | 0.906 | 0.982 | 1.059 | 1.072 | 0.997 | 0.742 | 1.035 | 0.898 |
| Ca | 0.027 | 0.033 | 0.024 | 0.041 | 0.031 | 0.030 | 0.023 | 0.037 | 0.036 | 0.029 | 0.034 |
| Na | 0 | 0.001 | 0.004 | 0.001 | 0.001 | 0.001 | 0.001 | 0.001 | 0.002 | 0.001 | 0.003 |
| Total | 4.000 | 3.995 | 4.010 | 4.003 | 4.004 | 4.001 | 3.999 | 4.008 | 3.996 | 3.997 | 4.013 |
| $X_{Mg}$ | 0.582 | 0.529 | 0.697 | 0.473 | 0.505 | 0.545 | 0.555 | 0.513 | 0.388 | 0.537 | 0.461 |
| $\sigma_{n-1}$ | 0 | 0.015 | 0 | 0 | 0.013 | 0.006 | 0.002 | 0 | 0.004 | 0.006 | 0 |

FeO = Fe(tot); $X_{Mg}$ = Mg/(Mg + Fe); Cation numbers on the basis of 6 (O).
*wt%* = weight percentage oxides; *a.f.u.* = atoms per formula unit.

*Table 2b.* Mineral analyses of clinopyroxene

| | Metavolcanic rocks | | | | Leuconorites/Hypersthene-bearing tonalites | | | | | | |
|---|---|---|---|---|---|---|---|---|---|---|---|
| Ref. | HW | HW | HW | HW | HW | DU | DU | HW | DU | DU | HW |
| No. | 141.1 | 013 | 043 | 143.6 | 035 | 137 | 115 | 147 | 72 | 105 | 047 |
| $SiO_2$ *(wt%)* | 52.74 | 52.23 | 53.69 | 51.99 | 52.10 | 52.13 | 52.53 | 52.48 | 51.73 | 52.44 | 51.60 |
| $Al_2O_3$ | 1.08 | 1.00 | 1.05 | 1.40 | 0.87 | 1.05 | 1.06 | 0.78 | 0.72 | 1.04 | 1.09 |
| $TiO_2$ | 0.20 | 0.19 | 0.26 | 0.25 | 0.16 | 0.18 | 0.12 | 0.08 | 0.10 | 0.10 | 0.14 |
| Fe | 9.71 | 11.42 | 6.07 | 13.09 | 11.78 | 11.35 | 11.84 | 11.70 | 15.72 | 11.29 | 14.21 |
| Mn | 0.34 | 0.24 | 0.25 | 0.35 | 0.24 | 0.22 | 0.38 | 0.35 | 0.42 | 0.38 | 0.30 |
| MgO | 13.63 | 12.54 | 15.55 | 11.35 | 12.10 | 12.87 | 12.64 | 12.60 | 9.86 | 12.44 | 11.52 |
| CaO | 21.54 | 21.85 | 22.71 | 21.75 | 22.34 | 21.65 | 20.24 | 21.81 | 20.83 | 21.56 | 21.03 |
| $Na_2O$ | 0.23 | 0.18 | 0.22 | 0.28 | 0.20 | 0.34 | 0.54 | 0.36 | 0.36 | 0.53 | 0.23 |
| Tot. | 99.47 | 99.65 | 99.80 | 100.46 | 99.79 | 99.79 | 99.35 | 100.16 | 99.74 | 99.78 | 100.12 |
| Si *(a.f.u.)* | 1.981 | 1.977 | 1.980 | 1.967 | 1.976 | 1.970 | 1.990 | 1.980 | 1.993 | 1.981 | 1.967 |
| Al | 0.048 | 0.045 | 0.046 | 0.063 | 0.039 | 0.047 | 0.047 | 0.035 | 0.033 | 0.046 | 0.049 |
| Ti | 0.005 | 0.005 | 0.007 | 0.007 | 0.005 | 0.005 | 0.003 | 0.002 | 0.003 | 0.003 | 0.004 |
| Fe | 0.305 | 0.361 | 0.187 | 0.414 | 0.374 | 0.359 | 0.375 | 0.369 | 0.506 | 0.357 | 0.453 |
| Mn | 0.011 | 0.008 | 0.008 | 0.011 | 0.008 | 0.007 | 0.012 | 0.011 | 0.014 | 0.012 | 0.010 |
| Mg | 0.763 | 0.707 | 0.855 | 0.640 | 0.684 | 0.725 | 0.714 | 0.709 | 0.556 | 0.701 | 0.655 |
| Ca | 0.867 | 0.886 | 0.897 | 0.882 | 0.908 | 0.877 | 0.821 | 0.882 | 0.860 | 0.873 | 0.859 |
| Na | 0.017 | 0.013 | 0.017 | 0.020 | 0.015 | 0.025 | 0.040 | 0.026 | 0.027 | 0.039 | 0.017 |
| Tot. | 3.997 | 4.002 | 3.997 | 4.004 | 4.009 | 4.015 | 4.002 | 4.014 | 3.992 | 4.012 | 4.014 |
| $X_{Mg}$ | 0.714 | 0.662 | 0.820 | 0.607 | 0.647 | 0.669 | 0.656 | 0.658 | 0.524 | 0.663 | 0.591 |
| $\sigma_{n-1}$ | 0 | 0.012 | 0 | 0 | 0.039 | 0.009 | 0.012 | 0 | 0.004 | 0 | 0 |

FeO = Fe(tot); $X_{Mg}$ = Mg/(Mg + Fe); Cation numbers on the basis of 6 (O).
*wt%* = weight percentage oxides; *a.f.u.* = atoms per formula unit.

Ti (Ti-Al$^{VI}$ exchange reaction: Indares & Martignole 1985, Schreurs 1985b).

### *Cordierite*

Both poikiloblastic and inclusion-free cordierites were analysed. They show no significant compositional differences. Cordierites have relatively homogeneous core compositions with $X_{Mg}$ varying between 0.507 and 0.687. Comparison of analyses of core and rim composition often shows a small increase in $X_{Mg}$ towards the rim (outer 100–150 $\mu$m), especially when in contact with garnet.

*Table 3.* Mineral analyses of garnet-orthopyroxene-bearing metavolcanic rocks

| | Garnet | | | Biotite | | | Orthopyroxene | | | Plagioclase | | |
|---|---|---|---|---|---|---|---|---|---|---|---|---|
| Ref. | HW | HW | HW | HW | HW | HW | HW | HW | HW | HW | HW | HW |
| No | 041 | 137.3 | 138.4 | 041 | 137.3 | 138.4 | 041 | 137.3 | 138.4 | 041 | 137.3 | 138.4 |
| $SiO_2$ *(wt%)* | 38.19 | 37.68 | 37.86 | 34.81 | 35.30 | 36.75 | 49.65 | 48.72 | 50.65 | 48.66 | 58.06 | 59.47 |
| $Al_2O_3$ | 21.23 | 21.14 | 21.33 | 15.03 | 14.54 | 15.30 | 1.20 | 1.23 | 1.38 | 32.29 | 26.20 | 25.26 |
| $TiO_2$ | | | | 4.53 | 4.56 | 3.15 | 0.15 | 0.14 | 0.09 | | | |
| FeO | 31.85 | 33.59 | 33.78 | 22.42 | 22.78 | 20.13 | 36.47 | 37.81 | 32.86 | | | |
| MnO | 1.17 | 1.46 | 1.82 | 0.00 | 0.04 | 0.00 | 0.51 | 0.59 | 0.51 | | | |
| MgO | 3.83 | 3.45 | 4.18 | 8.36 | 8.77 | 10.97 | 11.83 | 11.25 | 14.60 | | | |
| CaO | 4.93 | 3.09 | 2.24 | 0.06 | 0.01 | 0.01 | 0.37 | 0.42 | 0.30 | 15.99 | 8.44 | 7.89 |
| BaO | | | | 1.74 | 0 | 0.30 | | | | | | |
| $Na_2O$ | | | | 0.04 | 0.06 | 0.05 | 0.02 | 0.00 | 0.02 | 2.54 | 6.71 | 7.15 |
| $K_2O$ | | | | 8.76 | 9.68 | 9.70 | | | | 0.05 | 0.22 | 0.11 |
| F | | | | 0.56 | 0 | 0.51 | | | | | | |
| sum | | | | 96.31 | 95.74 | 96.86 | | | | | | |
| – O = F | | | | 0.26 | 0 | 0.24 | | | | | | |
| Total | 101.20 | 100.45 | 101.21 | 96.05 | 95.74 | 96.62 | 100.20 | 100.16 | 100.41 | 99.53 | 99.63 | 99.88 |
| Si *(a.f.u.)* | 3.003 | 3.002 | 2.991 | 5.444 | 5.485 | 5.582 | 1.978 | 1.959 | 1.975 | 2.237 | 2.608 | 2.657 |
| Al | 1.968 | 1.986 | 1.986 | 2.780 | 2.664 | 2.738 | 0.056 | 0.058 | 0.063 | 1.749 | 1.387 | 1.330 |
| Ti | | | | 0.533 | 0.530 | 0.360 | 0.004 | 0.004 | 0.003 | | | |
| Fe | 2.095 | 2.238 | 2.232 | 2.932 | 2.961 | 2.557 | 1.215 | 1.272 | 1.071 | | | |
| Mn | 0.078 | 0.098 | 0.122 | 0.000 | 0.005 | 0.000 | 0.017 | 0.020 | 0.017 | | | |
| Mg | 0.449 | 0.409 | 0.492 | 1.948 | 2.031 | 2.483 | 0.702 | 0.674 | 0.848 | | | |
| Ca | 0.415 | 0.264 | 0.189 | 0.009 | 0.002 | 0.002 | 0.016 | 0.018 | 0.012 | 0.787 | 0.406 | 0.378 |
| Ba | | | | 0.106 | 0 | 0.018 | | | | | | |
| Na | | | | 0.011 | 0.017 | 0.016 | 0.002 | 0.000 | 0.001 | 0.226 | 0.584 | 0.620 |
| K | | | | 1.748 | 1.919 | 1.879 | | | | 0.003 | 0.012 | 0.006 |
| F | | | | 0.278 | 0 | 0.243 | | | | | | |
| Total | 8.008 | 7.997 | 8.012 | 15.789 | 15.614 | 15.878 | 3.990 | 4.005 | 3.990 | 5.002 | 4.997 | 4.991 |
| $X_{Mg}$ | 0.176 | 0.155 | 0.181 | 0.399 | 0.047 | 0.488 | 0.366 | 0.346 | 0.442 | | | |
| $X_{An}$ | | | | | | | | | | 0.775 | 0.405 | 0.376 |
| $X_{Py}$ | 0.15 | 0.13 | 0.16 | | | | | | | | | |
| $X_{Alm}$ | 0.69 | 0.74 | 0.74 | | | | | | | | | |
| $X_{Sp}$ | 0.03 | 0.03 | 0.04 | | | | | | | | | |
| $X_{Gr}$ | 0.13 | 0.09 | 0.06 | | | | | | | | | |

FeO = Fe (total); $X_{Mg}$ = Mg/(Mg Fe); $X_{an}$ = Ca/(Ca + Na + K); $X_{Py}$ = Mg/(Mg + Fe + Ca + Mn); $X_{Alm}$ = Fe/(Mg + Fe + Ca + Mn); $X_{Sp}$ = Mn/(Mg + Fe + Mn + Ca); $X_{Gr}$ = Ca/(Mg + Fe + Mn + Ca).

Cation numbers on the basis of 12 (O) for garnet, 22 (O) for biotite, 6 (O) for orthopyroxene, and 8 (O) for plagioclase. *wt%* = weight percentage oxides; *a.f.u.* = atoms per formula unit.

### Plagioclase

Most plagioclase grains are homogeneous, but some zoning occurs. In pelitic gneisses, the anorthite content varies between 22 and 31%. The plagioclase in metavolcanic rocks has a much higher anorthite content (38–88%).

### Orthopyroxene

The orthopyroxene (opx) compositions are near hypersthene. They are rich in Fe and Mn, and contain small amounts of Ca and Mg (≈ 0.70 wt%).

In metavolcanic rocks, orthopyroxenes coexisting with garnet have much higher Fe and lower Mg contents ($X_{Mg}$(opx) = 0.346-0.442) than orthopyroxenes coexisting with clinopyroxene ($X_{Mg}$ (opx) = 0.473–0.697). This is probably related to rock composition and mineralogy. They are also relatively low in Ca and Mn, both elements being more easily incorporated in the garnet. Orthopyroxenes occurring in charnockitic rocks have a Fe-Mg composition intermediate between the former two ($X_{Mg}$(opx) = 0.388–0.555).

Rims of orthopyroxenes (outer 100 $\mu$m) in contact with clinopyroxene have less Ca and more Fe, probably due to Ca-Fe-Mg reequilibration during cooling. The opposite is found in clinopyroxene (see below).

### Clinopyroxene

Clinopyroxenes plot near the diopside-hedenbergite join. They are Ca-rich with moderately variable amounts of Fe and Mg ($X_{Mg}$ = 0.422–0.670). Clinopyroxenes from charnockitic rocks have a lower $X_{Mg}$ (0.524–0.669) than clinopyroxenes from metavolcanic rocks ($X_{Mg}$ = 0.607–0.820). Clinopy-

*Table 4a.* Mineral analyses pelitic gneisses: garnet

| Ref.<br>No. | CN<br>151 | CN<br>153 | CN<br>133 | CN<br>83 | CN<br>139 | CN<br>143 | HW<br>166 | HW<br>140.6 | HW<br>138.6 | HW<br>143.10 | CN<br>87b | CN<br>90 |
|---|---|---|---|---|---|---|---|---|---|---|---|---|
| $SiO_2$ *(wt%)* | 37.95 | 38.13 | 37.82 | 37.84 | 37.86 | 37.71 | 38.42 | 37.97 | 37.55 | 37.56 | 38.62 | 37.52 |
| $Al_2O_3$ | 21.37 | 21.69 | 21.60 | 21.41 | 21.38 | 21.48 | 21.36 | 21.20 | 21.20 | 21.40 | 21.76 | 21.32 |
| FeO | 29.17 | 34.54 | 35.66 | 34.11 | 34.94 | 34.02 | 32.14 | 34.09 | 33.98 | 34.90 | 33.64 | 37.14 |
| MnO | 6.32 | 1.45 | 0.82 | 1.12 | 1.31 | 0.90 | 0.61 | 0.66 | 1.65 | 2.17 | 1.54 | 1.14 |
| MgO | 3.26 | 5.05 | 4.30 | 4.93 | 4.50 | 5.21 | 6.35 | 5.17 | 4.10 | 3.62 | 4.95 | 3.06 |
| CaO | 2.41 | 0.67 | 0.93 | 1.09 | 0.87 | 0.89 | 0.99 | 1.01 | 1.84 | 1.22 | 1.09 | 1.02 |
| Total | 100.39 | 101.53 | 101.13 | 100.50 | 100.86 | 100.21 | 99.87 | 100.10 | 100.32 | 100.87 | 101.60 | 101.20 |
| Si *(a.f.u.)* | 3.020 | 2.991 | 2.990 | 2.997 | 2.999 | 2.990 | 3.022 | 3.014 | 2.993 | 2.990 | 3.015 | 2.993 |
| Al | 2.004 | 2.005 | 2.013 | 1.998 | 1.996 | 2.007 | 1.980 | 1.991 | 1.992 | 2.008 | 2.002 | 2.004 |
| Fe | 1.941 | 2.266 | 2.358 | 2.259 | 2.315 | 2.256 | 2.115 | 2.243 | 2.265 | 2.323 | 2.196 | 2.478 |
| Mn | 0.420 | 0.098 | 0.055 | 0.075 | 0.088 | 0.060 | 0.040 | 0.044 | 0.112 | 0.146 | 0.102 | 0.077 |
| Mg | 0.387 | 0.590 | 0.507 | 0.582 | 0.531 | 0.616 | 0.744 | 0.606 | 0.488 | 0.429 | 0.576 | 0.364 |
| Ca | 0.205 | 0.056 | 0.079 | 0.092 | 0.074 | 0.076 | 0.084 | 0.085 | 0.157 | 0.104 | 0.091 | 0.087 |
| Total | 7.977 | 8.006 | 8.002 | 8.003 | 8.003 | 8.005 | 7.985 | 7.983 | 8.007 | 8.000 | 7.982 | 8.003 |
| $X_{Mg}$ | 0.166 | 0.207 | 0.177 | 0.205 | 0.187 | 0.219 | 0.260 | 0.162 | 0.177 | 0.156 | 0.208 | 0.128 |
| $\sigma_{n-1}$ | 0 | 0.009 | 0.009 | 0.015 | 0.011 | 0.006 | 0 | 0 | 0 | 0 | 0.007 | 0.007 |
| $X_{Py}$ | 0.13 | 0.20 | 0.17 | 0.19 | 0.18 | 0.20 | 0.25 | 0.20 | 0.16 | 0.14 | 0.19 | 0.12 |
| $X_{Alm}$ | 0.66 | 0.75 | 0.79 | 0.75 | 0.77 | 0.75 | 0.71 | 0.76 | 0.75 | 0.77 | 0.74 | 0.82 |
| $X_{Sp}$ | 0.14 | 0.03 | 0.02 | 0.02 | 0.03 | 0.02 | 0.03 | 0.01 | 0.04 | 0.03 | 0.03 | 0.03 |
| $X_{Gr}$ | 0.07 | 0.02 | 0.03 | 0.03 | 0.02 | 0.03 | 0.03 | 0.03 | 0.05 | 0.03 | 0.03 | 0.03 |

FeO = Fe (total); $X_{Mg}$ = Mg/(Mg + Fe); Cation numbers on the basis of 12 (O). *wt%* = weight percentage oxides; *a.f.u.* = atoms per formula unit. $X_{Py}$, $X_{Alm}$, $X_{Sp}$ and $X_{Gr}$ as in Table 3.

roxene in contact with orthopyroxene contains more Ca and less Fe compared to matrix clinopyroxene.

## Thermobarometric results

Various independent geothermobarometric methods were applied to samples selected from the amphibolite and granulite facies domains and from the transition zone. Analyses of cores of isolated grains were used for calculating peak metamorphic temperatures. The thermobarometric results obtained through the conventional methods, which were used for peak metamorphic estimates, are shown in Tables 5a–c. The variation in temperature estimates derived from $\sigma_{n-1}$ for the average $X_{Mg}$ values presented in Tables 2 to 4 is ± 30° C, which remains within the error limits (± 50° C) of the thermometric calculations. The temperatures and pressures printed in italics in Tables 5a–c are indicated in Fig. 5. Other calibrations frequently used in literature are given for comparison. Results obtained with GEO-CALC, used to obtain an indication of the P-T path, are shown in Fig. 4.

*Table 4b*. Mineral analyses pelitic gneisses: biotite

| Ref. No. | CN 151 | CN 153 | CN 133 | CN 83 | CN 139 | CN 143 | HW 166 | HW 140.6 | HW 138.6 | HW 143.10 | CN 87b | CN 90 |
|---|---|---|---|---|---|---|---|---|---|---|---|---|
| $SiO_2$ *(wt%)* | 34.46 | 35.08 | 35.10 | 34.74 | 34.79 | 35.18 | 36.66 | 36.38 | 35.90 | 35.59 | 35.82 | 34.34 |
| $Al_2O_3$ | 15.43 | 18.57 | 18.05 | 18.07 | 17.93 | 17.07 | 17.28 | 17.11 | 16.45 | 15.60 | 18.26 | 18.53 |
| $TiO_2$ | 2.32 | 2.51 | 3.12 | 3.47 | 3.44 | 3.64 | 4.05 | 4.16 | 2.95 | 4.35 | 2.94 | 3.59 |
| FeO | 19.95 | 17.59 | 19.13 | 20.07 | 19.37 | 18.34 | 17.28 | 17.60 | 19.54 | 20.79 | 19.21 | 21.50 |
| MnO | 0.24 | 0.03 | 0 | 0.06 | 0.04 | 0.02 | 0.03 | 0.04 | 0.05 | 0.11 | 0.07 | 0.05 |
| MgO | 10.25 | 10.54 | 9.53 | 8.97 | 8.99 | 10.46 | 10.69 | 10.15 | 10.46 | 9.92 | 9.64 | 7.20 |
| BaO | 0.22 | 0.05 | 0.13 | 0.13 | 0.12 | 0.11 | 0 | 0 | 0 | 0 | 0.52 | 0.12 |
| $Na_2O$ | 0.14 | 0.22 | 0.13 | 0.14 | 0.12 | 0.11 | 0.09 | 0.09 | 0.05 | 0.04 | 0.06 | 0.15 |
| $K_2O$ | 8.91 | 9.46 | 9.73 | 9.63 | 9.60 | 9.52 | 10.03 | 9.89 | 9.91 | 9.50 | 8.63 | 9.34 |
| F | 0.55 | 0.44 | 0.73 | 0.30 | 0.47 | 0.83 | 0.44 | 0.76 | 0.66 | 1.66 | 0.31 | 0.57 |
| sum | 92.47 | 94.49 | 95.65 | 95.58 | 94.87 | 95.28 | 96.55 | 96.18 | 95.97 | 97.56 | 95.49 | 95.39 |
| − O = F | 0.23 | 0.19 | 0.31 | 0.13 | 0.20 | 0.35 | 0.21 | 0.36 | 0.31 | 0.79 | 0.13 | 0.24 |
| Total | 92.24 | 94.30 | 95.34 | 95.45 | 94.67 | 94.93 | 96.34 | 95.82 | 95.66 | 96.77 | 95.33 | 95.15 |
| Si *(a.f.u.)* | 5.465 | 5.348 | 5.336 | 5.317 | 5.344 | 5.352 | 5.491 | 5.499 | 5.497 | 5.450 | 5.429 | 5.288 |
| Al | 2.884 | 3.337 | 3.234 | 3.259 | 3.246 | 3.061 | 3.051 | 3.049 | 2.969 | 2.815 | 3.262 | 3.363 |
| Ti | 0.277 | 0.288 | 0.357 | 0.399 | 0.397 | 0.416 | 0.457 | 0.473 | 0.339 | 0.501 | 0.335 | 0.416 |
| Fe | 2.646 | 2.243 | 2.432 | 2.569 | 2.488 | 2.334 | 2.167 | 2.225 | 2.502 | 2.662 | 2.435 | 2.769 |
| Mn | 0.032 | 0.004 | 0 | 0.008 | 0.005 | 0.003 | 0.003 | 0.005 | 0.007 | 0.014 | 0.009 | 0.007 |
| Mg | 2.423 | 2.395 | 2.159 | 2.046 | 2.058 | 2.372 | 2.386 | 2.285 | 2.387 | 2.264 | 2.178 | 1.675 |
| Ba | 0.014 | 0.003 | 0.008 | 0.008 | 0.007 | 0.007 | 0 | 0 | 0 | 0 | 0.031 | 0.007 |
| Na | 0.043 | 0.065 | 0.038 | 0.042 | 0.036 | 0.033 | 0.026 | 0.026 | 0.016 | 0.011 | 0.018 | 0.042 |
| K | 1.803 | 1.840 | 1.887 | 1.880 | 1.881 | 1.848 | 1.917 | 1.908 | 1.936 | 1.856 | 1.669 | 1.835 |
| F | 0.276 | 0.212 | 0.351 | 0.145 | 0.228 | 0.399 | 0.208 | 0.365 | 0.319 | 0.804 | 0.149 | 0.278 |
| Total | 15.863 | 15.734 | 15.802 | 15.673 | 15.690 | 15.825 | 15.706 | 15.835 | 15.972 | 16.377 | 15.515 | 15.680 |
| $X_{Mg}$ | 0.478 | 0.516 | 0.470 | 0.443 | 0.453 | 0.504 | 0.524 | 0.506 | 0.488 | 0.460 | 0.472 | 0.377 |
| $\sigma_{n-1}$ | 0 | 0.030 | 0.012 | 0.005 | 0.004 | 0.010 | 0 | 0 | 0 | 0 | 0.007 | 0.006 |

FeO = Fe (total); $X_{Mg}$ = Mg/(Mg + Fe); Cation numbers on the basis of 22 (O).
*wt%* = weight percentage oxides; *a.f.u.* = atoms per formula unit.

### *Thermometry*

#### *Two-pyroxene*

Pyroxene thermometry is often used as the geothermometric method in granulite facies domains. Different two-pyroxene thermometers have been developed, using the temperature dependent solvus (Lindsley 1983, Nabelek et al. 1987), Fe-Mg exchange (Wood & Banno 1973, Wells 1977, Kretz 1982), or Ca-transfer reactions (Kretz 1982).

For the two-pyroxene-bearing metavolcanic and charnockitic rocks the thermometers of Kretz-Ca (< 1080° C) (1982), Kretz-Mg-Fe (1982), Wells (1977) and Wood & Banno (1973) were used (Table 5a). Temperature estimates for the Kretz thermometers are between 670 and 820° C, the lower temperatures being interpreted as re-equilibrated values due to redistribution of Mg, Fe and Ca. Orthopyroxenes in the re-equilibrated samples show much more alteration to uralite along cracks and cleavage planes.

The Wells (1977) and Wood & Banno (1973) thermometers, often used in granulite terrains, give an overestimation of the order of 100 to 200° C for the Turku granulites, consistent with similar studies in other granulite areas (Bohlen & Essene 1979). The Wells thermometer (1977) gives the best results for ultramafic rocks at temperatures > 900° C, and erroneously high temperatures for (Fe-rich) granulites (650–850° C; Bohlen & Essene 1979, Essene 1982, Perkins et al. 1982).

Both thermometers of Kretz (1982), discrimi-

*Table 4c.* Mineral analyses pelitic gneisses: cordierite, spinel and plagioclase

| | Cordierite | | | | | | | Spinel | Plagioclase | | | | | | |
|---|---|---|---|---|---|---|---|---|---|---|---|---|---|---|---|
| Ref. | CN | CN | CN | CN | HW | HW | CN | HW | CN | CN | CN | CN | HW | HW | CN |
| No. | 133 | 83 | 139 | 143 | 166 | 140.6 | 90 | 166 | 153 | 83 | 139 | 143 | 166 | 140.6 | 90 |
| $SiO_2$ *(wt%)* | 47.99 | 48.57 | 47.50 | 47.69 | 49.10 | 49.08 | 47.48 | | 61.75 | 62.56 | 61.27 | 61.71 | 62.26 | 61.47 | 60.85 |
| $Al_2O_3$ | 32.46 | 32.52 | 31.96 | 32.08 | 32.10 | 32.67 | 32.19 | 59.04 | 22.84 | 23.34 | 23.38 | 23.00 | 24.02 | 24.35 | 24.72 |
| FeO | 9.10 | 8.50 | 9.24 | 8.84 | 7.15 | 8.13 | 10.59 | 33.07 | | | | | | | |
| MnO | 0.07 | 0.10 | 0.10 | 0.07 | 0.01 | 0.04 | 0.11 | 0.04 | | | | | | | |
| MgO | 7.67 | 7.50 | 7.66 | 7.89 | 8.82 | 8.25 | 6.12 | 4.27 | | | | | | | |
| ZnO | | | | | | | | 2.77 | | | | | | | |
| CaO | 0.02 | 0.01 | 0.05 | 0.01 | 0.03 | 0.01 | 0.02 | | 4.58 | 4.70 | 5.33 | 4.99 | 5.57 | 5.69 | 6.73 |
| $Na_2O$ | 0.18 | 0.08 | 0.17 | 0.12 | 0.11 | 0.09 | 0.18 | | 9.05 | 8.68 | 8.50 | 8.39 | 8.47 | 8.37 | 7.77 |
| $K_2O$ | | | | | | | | | 0.23 | 0.18 | 0.27 | 0.27 | 0.23 | 0.13 | 0.16 |
| Total | 97.49 | 97.28 | 96.68 | 96.70 | 97.32 | 98.27 | 97.05 | 99.19 | 98.45 | 99.46 | 98.75 | 98.36 | 100.55 | 100.01 | 100.23 |
| Si *(a.f.u.)* | 5.003 | 5.051 | 5.001 | 5.007 | 5.043 | 5.044 | 5.040 | | 2.779 | 2.781 | 2.753 | 2.777 | 2.747 | 2.727 | 2.706 |
| Al | 3.988 | 3.986 | 3.966 | 3.970 | 3.956 | 3.958 | 3.997 | 1.981 | 1.212 | 1.223 | 1.238 | 1.220 | 1.249 | 1.274 | 1.296 |
| Fe | 0.793 | 0.739 | 0.814 | 0.776 | 0.614 | 0.699 | 0.933 | 0.787 | | | | | | | |
| Mn | 0.006 | 0.009 | 0.009 | 0.006 | 0.001 | 0.003 | 0.010 | 0.001 | | | | | | | |
| Mg | 1.192 | 1.163 | 1.202 | 1.235 | 1.350 | 1.263 | 0.961 | 0.181 | | | | | | | |
| Zn | | | | | | | | 0.058 | | | | | | | |
| Ca | 0.002 | 0.003 | 0.006 | 0.001 | 0.003 | 0.001 | 0.002 | | 0.221 | 0.224 | 0.257 | 0.241 | 0.263 | 0.271 | 0.304 |
| Na | 0.036 | 0.016 | 0.035 | 0.025 | 0.021 | 0.018 | 0.037 | | 0.792 | 0.750 | 0.743 | 0.734 | 0.724 | 0.720 | 0.672 |
| K | | | | | | | | | 0.013 | 0.010 | 0.015 | 0.016 | 0.013 | 0.007 | 0.009 |
| Total | 11.020 | 10.967 | 11.033 | 11.020 | 10.988 | 10.986 | 10.980 | 3.009 | 5.017 | 4.988 | 5.006 | 4.988 | 4.996 | 4.999 | 4.987 |
| $X_{Mg}$ | 0.601 | 0.611 | 0.596 | 0.614 | 0.687 | 0.644 | 0.507 | 0.187 | | | | | | | |
| $X_{An}$ | | | | | | | | | 0.215 | 0.228 | 0.253 | 0.243 | 0.263 | 0.272 | 0.309 |
| $\sigma_{n-1}$ | 0.011 | 0.013 | 0.004 | 0.003 | 0 | 0 | 0.009 | 0 | 0 | 0.018 | 0.005 | 0.008 | 0 | 0 | 0 |

FeO = Fe (total); $X_{Mg}$ = Mg/(Mg + Fe); $X_{An}$ = Ca/(Ca + Na + Ca); Cation numbers on the basis of 18 (O) for cordierite, on the basis of 4 (O) for spinel and on the basis of 8(O) for plagioclase. *wt%* = weight percentage oxides; *a.f.u.* = atoms per formula unit.

nated for metamorphic (<1080° C) and igneous rocks (>1080° C), yield lower temperatures. These are in agreement with temperatures obtained with garnet-biotite and garnet-cordierite thermometry (see next sections) and correspond better with the geological observations.

*Garnet-orthopyroxene*

The garnet-orthopyroxene thermometers of Harley (1984), Mori & Green (1978), Sen & Bhattacharya (1984), and Wood (1974) were applied to three samples of the Turku area (Table 5b). When compared with two-pyroxene, garnet-biotite, and garnet-cordierite thermometers, only the thermometer of Harley (1984) yields more or less similar temperatures, probably because only this one is calibrated for the appropriate rocks.

Temperatures of 755, 705 and 590° C were obtained for the three investigated samples. The 590° C temperature is considered to represent a disequilibrium value due to retrogression, consistent with the similarly low temperature yielded by the garnet-biotite thermometer.

*Garnet-cordierite*

The garnet-cordierite thermometers of Thompson (1976), Holdaway & Lee (1977), and Perchuk & Lavrent'eva (1983) were all applied (Table 5c). The latter thermometer yields temperature estimates in the range from 680 to 725° C in the transition zone and from 720 to 740° C in the granulite domain. Perchuk & Lavrent'eva (1983), in their experimentally determined calibration, used garnets and cordierites with compositions corresponding to those in natural granulite facies assemblages. They obtained very consistent $K_D$ (= distribution coefficient of elements between certain minerals) values with temperatures over a wide range of $X_{Mg}$ for cordierite and garnet. This results in a reliable thermometer for a temperature range from 550 to 1000° C.

The thermometers of Thompson (1976) and Holdaway & Lee (1977) give slightly higher (5 to 40° C) temperatures. Their calibrations are heavily weighted towards lower temperatures and extrapolated to higher temperatures. This results in larger errors at high temperature.

*Garnet-biotite*

The garnet-biotite thermometers of Holdaway & Lee (1977), Ferry & Spear (1978), Perchuk & Lavrent'eva (1983) and Perchuk & Aranovich (1986) were applied to pelitic gneisses and garnet-orthopyroxene-bearing metavolcanic rocks (Tables 5b, c). Temperatures calculated according to Perchuk & Aranovic (1986) give 650–680° C for the amphibolite domain, 675–725° C for the transition zone, and 715–740° C for the granulite facies domain. The other thermometers (Holdaway & Lee 1977, Ferry & Spear 1978, Perchuk & Lavrent'eva 1983) give in general similar results, but they produce deviations of up to 100° C in some samples (Ferry & Spear 1978).

Temperatures obtained with the thermometer of Ferry & Spear (1978) are consistently higher, showing an increase in temperature difference with increasing metamorphic grade.

Perchuk & Lavrent'eva (1983) applied the same experimental method which they used for their garnet-cordierite thermometer. Contrary to this thermometer, they failed to produce biotites and garnets with a large variance in $X_{Mg}$ at all desired temperatures. Instead, they considered an ideal distribution of Fe and Mg between these minerals at temperatures higher than 600° C based on earlier studies (Thompson 1976, Holdaway & Lee 1977). This results in a temperature underestimation.

Perchuk & Aranovich (1986) included a correction for the influence of fluorine in their thermometer. They state that introduction of fluorine into biotite in the position of the OH group strongly affects the equilibrium with other minerals, especially with garnet. Fluorine has a very high chemical affinity to Mg, and shifts the equilibrium of the reaction to lower temperatures. Temperature calculations for sample HW143.10 (1.66 wt% F) clearly demonstrate the influence of fluorine on temperature. Temperatures obtained through the other methods are 65 to 185° C lower for the same sample.

*Barometry*

*Garnet-orthopyroxene-plagioclase-quartz*
Garnet and orthopyroxene coexist only in a few samples in the Turku area (Table 5b). Application of garnet-orthopyroxene-plagioclase-quartz barometry according to Perkins & Chipera (1985) leads to pressure estimates of 4.6–5.2 kbar for the Fe-reaction and 4.9–8.2 kbar for the Mg-reaction. Perkins & Chipera (1985) state that for Fe-rich rocks ($X_{Fe}$(opx) ≥ 0.5) a discrepancy occurs between the two barometers, and that the Fe-based barometer should be preferred. Deviation of the Mg-based barometer is probably due to errors in activity models for garnet and/or orthopyroxene (Perkins & Chipera 1985). Only for sample HW138.4 ($X_{Fe}$(opx) = 0.538) the two barometers give broadly consistent results ($P_{Fe}$ = 4.6 kbar and $P_{Mg}$ = 4.9 kbar).

Perkins & Chipera (1985) recalculated the barometer of Newton & Perkins (1982) using a different activity model for garnet. Pressures estimated with this recalculated barometer, based on the Mg-reaction, vary from 4.0 to 5.0 kbar. For sample HW138.4 their barometer gives a much lower pressure of 2.5 kbar, which is probably due to the low Ca content in both the garnet and the orthopyroxene.

*Garnet-cordierite-sillimanite-quartz*
Most pelitic gneisses in the transition zone and granulite domain contain the assemblage garnet-cordierite-sillimanite-quartz (Table 5b). Pressure estimates according to Aranovich & Podlesskii (1983) based on the Fe-reaction (Fe-cordierite = almandine + sillimanite + quartz) vary from 4.7 to 5.2 kbar. The Mg-reaction (Mg-cordierite = pyrope + sillimanite + quartz) gives pressures of 4.4 to 5.2 kbar. Large quantities of free sillimanite along the boundaries between garnet and cordierite (Fig. 3A) were only found in sample CN90 and are most likely a retrograde reaction product. The pressure for this sample was 4.3 kbar for the Fe-reaction and 3.9 kbar for the Mg-reaction.

Pressures calculated with the barometers of Holdaway & Lee (1977) and Newton & Wood (1979) are 0.5 to 1.0 kbar higher, giving 5.2–6.5 and 5.0–5.9 kbar respectively.

*Garnet-plagioclase-sillimanite-quartz*
This barometer, based on the regular distribution of Ca between plagioclase and garnet cores, was developed by Ghent (1976) and modified by Newton & Haselton (1981) and Perchuk (1986) (Table 5c). All pressures are calculated with Gamma $X^{Ca}$ according to Ghent & Stout (1981) at 750° C and $X_{H_2O}$ = 0.4 (maximum). The pressures calculated with the barometer of Perchuk (1986) vary between 4.0 and 5.2 kbar. The barometers of Ghent (1976) and Newton & Haselton (1981) give similar values. The pressures calculated with the barometer of Ghent (1976) are in general higher (0.5 kbar) than those calculated with the barometers of Newton & Haselton (1981) and Perchuk (1986). Pressures for samples CN90 and CN153 are considerably lower, 3.4 and 3.0 kbar respectively. The presence of andalusite in sample CN153 is another indication of lower P-T conditions.

*Calculation of P-T diagrams with the use of GEO-CALC*

Recently, the use of software programs based on thermodynamic mineral data, such as GEO-CALC, has become an additional tool for obtaining P-T estimates. In this study, the program PTX-SYSTEM of the software package GEO-CALC (Brown et al. 1987, 1988) was used to obtain P-T estimates for the post-peak metamorphic path. PTX-SYSTEM calculates complete pressure-temperature (P-T), temperature-composition (T-$X_{H_2O\text{-}CO_2}$), and pressure-composition (P-$X_{H_2O\text{-}CO_2}$) phase diagrams (Perkins et al. 1986, Berman et al. 1987, Brown et al. 1988) and uses the thermodynamic data set of Berman (1988) for minerals.

For garnet-cordierite gneisses, the reaction curves of almandine + phlogopite = pyrope + annite, grossular + aQuartz + sillimanite = 3 anorthite, and 2 pyrope + 5 aQuartz + 4 sillimanite = 3 cordierite were used to obtain the P-T conditions for a given mineral assemblage (Fig. 4A). The mutual positions of these curves can also be used as an

*Table 5a.* Thermometric results: Orthopyroxene-clinopyroxene-bearing metavolcanic rocks and leuconorites/hypersthene-bearing tonalites

| Orthopyroxene-clinopyroxene | | | | | | | | | | | |
|---|---|---|---|---|---|---|---|---|---|---|---|
| Ref.<br>no. | HW<br>035 | DU<br>137 | DU<br>115 | HW<br>147 | DU<br>72 | DU<br>105 | HW<br>141.1 | HW<br>0.13 | HW<br>0.43 | HW<br>0.47 | HW<br>1.43.6 |
| ***K-Ca*** | ***670*** | ***750*** | ***765*** | ***765*** | ***715*** | ***730*** | ***818*** | ***740*** | ***778*** | ***763*** | ***690*** |
| K-MgFe | 764 | 724 | 825 | 750 | 770 | 773 | 762 | 770 | 677 | 766 | 780 |
| Wells | 835 | 888 | 862 | 866 | 861 | 851 | 911 | 878 | 889 | 907 | 853 |
| W&B | 800 | 844 | 826 | 823 | 806 | 818 | 867 | 833 | 888 | 843 | 808 |

Calculated temperatures (in ° C) with the orthopyroxene-clinopyroxene thermometer. Temperatures respectively according to Kretz-Ca-≤ 1080° C and Kretz-Fe-Mg (1982), Wells (1977) and Wood & Banno (1973). Results in italics are mapped in Fig. 5.

*Table 5b.* Thermobarometric results: garnet-orthopyroxene-bearing metavolcanic rocks

| | Garnet-orthopyroxene | | | | Garnet-biotite | | | | | Gt-opx-plag-qtz | | |
|---|---|---|---|---|---|---|---|---|---|---|---|---|
| Ref.<br>no | ***H*** | M&G | S&B | W | H&L | F&S | I&M | P&L | ***P&A*** | ***P&C$_{Fe}$*** | P&C$_{Mg}$ | N&P |
| HW041 | ***755*** | 896 | 870 | 655 | 742 | 843 | 734 | 712 | ***742*** | ***5.2*** | 8.2 | 5.0 |
| HW137.3 | ***705*** | 824 | 790 | 628 | 683 | 742 | 625 | 666 | ***661*** | ***4.6*** | 7.2 | 4.0 |
| HW138.4 | ***590*** | 641 | 628 | 630 | 639 | 670 | 594 | 629 | ***656*** | ***4.6*** | 4.9 | 2.5 |

Temperatures (in ° C) calculated at 5 kbar for: garnet-orthopyroxene according to H: Harley (1984), M&G: Mori & Green (1978), S&B: Sen & Bhattacharya (1984) and W: Wood (1974); garnet-biotite according to Indares & Martignole (1985) (for other abbreviations see Table 5c).
Pressures (in kbar) calculated at 750° C for gt-opx-plag-qtz according to P&C$_{Fe}$ and P&C$_{Mg}$: Perkins & Chipera (1985) on Fe and Mg basis, respectively and N&P: Newton & Perkins (1982). Results in italics are mapped in Fig. 5.

*Table 5c.* Thermobarometric results: pelitic gneisses

| Ref.<br>No. | CN<br>151 | CN<br>153 | CN<br>133 | CN<br>83 | CN<br>139 | CN<br>143 | HW<br>166 | HW<br>140.6 | HW<br>138.6 | HW<br>143.10 | CN<br>87b | CN<br>90 |
|---|---|---|---|---|---|---|---|---|---|---|---|---|
| Thermometry | | | | | | | | | | | | |
| *Garnet-biotite T (° C)* | | | | | | | | | | | | |
| H&L | 628 | 658 | 656 | 743 | 695 | 685 | 739 | 679 | 637 | 627 | 712 | 657 |
| F&S | 653 | 701 | 698 | 845 | 761 | 746 | 838 | 736 | 668 | 652 | 790 | 699 |
| P&L | 595 | 647 | 649 | 714 | 676 | 672 | 714 | 669 | 630 | 620 | 688 | 649 |
| ***P&A*** | ***649*** | ***668*** | ***683*** | ***726*** | ***699*** | ***714*** | ***732*** | ***705*** | ***664*** | ***715*** | ***702*** | ***674*** |
| *Garnet-cordierite T (° C)* | | | | | | | | | | | | |
| Th | | | 713 | 762 | 743 | 781 | 754 | 729 | | | | 712 |
| H&L | | | 688 | 729 | 713 | 744 | 722 | 701 | | | | 687 |
| ***P&L*** | | | ***684*** | ***724*** | ***706*** | ***740*** | ***718*** | ***698*** | | | | ***682*** |
| Barometry | | | | | | | | | | | | |
| *Garnet-cordierite-sillimanite-quartz P (kbar)* | | | | | | | | | | | | |
| H&L | | | 5.9 | 5.9 | 5.8 | 5.9 | 6.5 | 6.2 | | | | 5.2 |
| N&W | | | 5.5 | 5.4 | 5.4 | 5.4 | 5.9 | 5.7 | | | | 5.0 |
| ***A&P$_{Fe}$*** | | | ***4.8*** | ***4.7*** | ***4.7*** | ***4.7*** | ***5.2*** | ***5.0*** | | | | ***4.3*** |
| A&P$_{Mg}$ | | | 4.4 | 4.7 | 4.5 | 4.9 | 5.2 | 4.7 | | | | 3.9 |
| *Garnet-plagioclase-sillimanite-quartz P (kbar)* | | | | | | | | | | | | |
| G | | 3.5 | | 4.6 | 4.5 | 5.3 | 5.5 | 4.8 | | | | 3.4 |
| N&H | | 3.1 | | 4.2 | 3.9 | 4.6 | 4.9 | 4.3 | | | | 3.0 |
| ***P*** | | ***3.0*** | | ***4.1*** | ***4.0*** | ***4.7*** | ***5.2*** | ***4.5*** | | | | ***3.4*** |

Calculated temperatures (in ° C) with the garnet-biotite thermometer at 5 kbar. Temperatures according to H&L: Holdaway & Lee (1977), F&S: Ferry & Spear (1978), P&L: Perchuk & Lavrent'eva (1983), P&A: Perchuk & Aranovich (1986), Th: Thompson (1976). Pressures (in kbar) calculated at 750° C with assumed $X_{H_2O} = 0.4$. Pressures according to H&L: Holdaway & Lee (1977); N&W: Newton & Wood (1979); A&P$_{FE}$: Aranovich & Podlesskii (1983) on Fe basis; A&P$_{Mg}$: Aranovich & Podlesskii (1983) on Mg basis; G: Ghent (1976); N&H: Newton & Haselton (1981) and P: Perchuk (1986). Results in italics are mapped in Fig. 5.

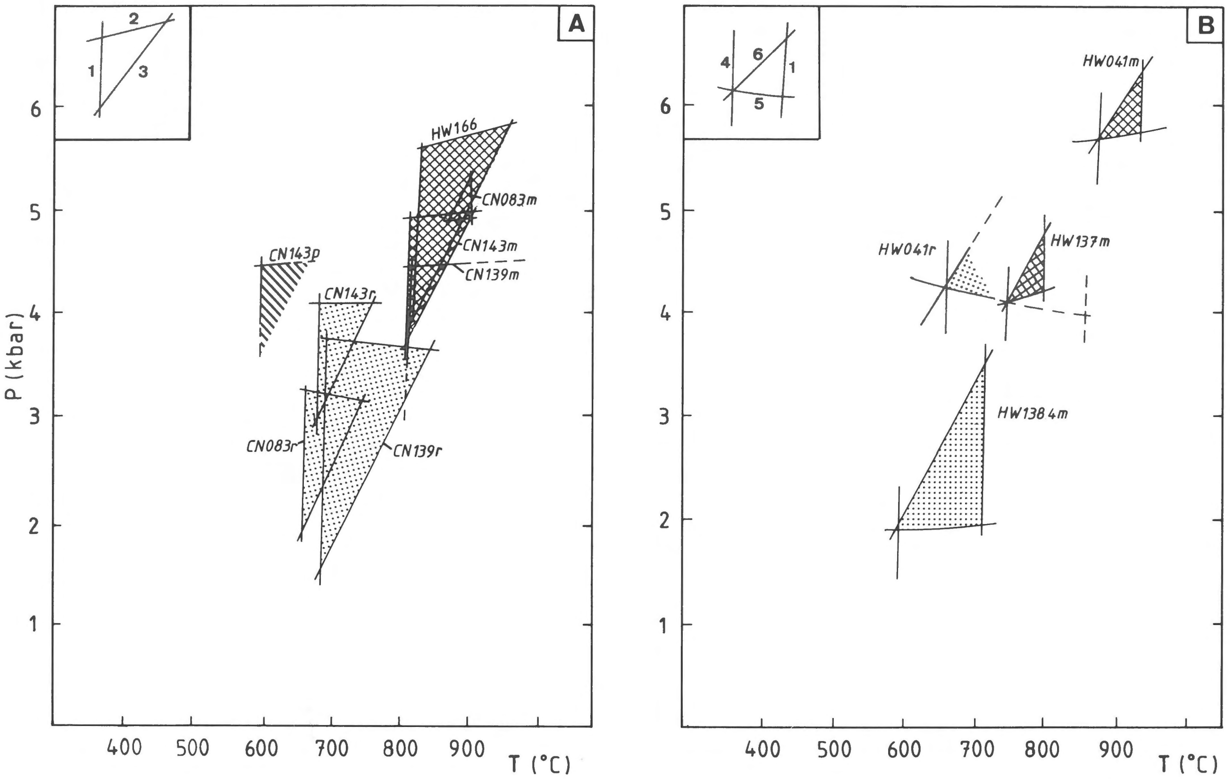

*Fig. 4.* Reaction curves for samples listed in Table 6, calculated with the software package of GEO-CALC using the thermodynamic data set of Berman (1988) for pelitic gneisses (A) and garnet-orthopyroxene-bearing metavolcanic rocks (B). Reaction curves: 1) Almandine + phlogopite = pyrope + annite; 2) Pyrope + 5 quartz + 4 sillimanite = 3 cordierite; 3) Grossular + quartz + 2 sillimanite = 3 anorthite; 4) 3 Enstatite + almandine = 3 ferrosilite + pyrope; 5) Grossular + 2 pyrope + 3 quartz = 6 enstatite + 3 anorthite; 6) 2 Almandine + grossular + 3 quartz = 6 ferrosilite + 3 anorthite.

indication of (dis)equilibrium for a specific mineral assemblage. Single mineral analyses were used instead of an average of several analyses per mineral as in conventional thermobarometry (Table 6).

The core and rim compositions of the selected minerals allow to restore possible P-T paths. The prograde stage can be estimated from biotite enclosed in garnet and from the Fe-richest core of garnet from garnet-cordierite gneisses. These minerals yield a P-T estimate of 610° C and 4.3 kbar. For peak metamorphic conditions the Mg-richest core of garnet and the Fe-richest matrix biotite were used, resulting in a temperature of 820° C and a pressure of 5 kbar. The Fe-richest rim of garnet and the Mg-richest biotite yielded a temperature of 670° C and a pressure of 3 kbar, representing the retrograde stage (Fig. 4A).

Using mineral analyses from orthopyroxene-garnet-bearing metavolcanic rocks (Table 6), similar results were obtained when applying curves of the reactions: almandine + phlogopite = pyrope + annite, 3 enstatite + almandine = 3 ferrosilite + pyrope, grossular + 2 pyrope + 3 quartz = 6 enstatite + 3 anorthite, and 2 almandine + grossular + 3 quartz = 6 ferrosilite + anorthite (Fig. 4B). This results in peak metamorphic conditions of 820° C at 5.5 kbar, and temperatures of 630° C at 3 kbar during retrogression (Fig. 4B).

## Discussion

### *P-T estimates*

### *Peak metamorphic conditions*

The combination of conventional geothermobarometry and P-T calculations with an internally consistent thermodynamic data set leads to consistent estimates of temperature and pressure. These estimates are 650–680° C and 4.8 $\mu$ 0.5 kbar for the amphibolite domain, 675–725° C and 4.7 ± 0.5 kbar for the transition zone, and 750 ± 50° C and 4.6–5.2 kbars for the granulite domain. The regional distribution of the estimates is shown in Fig. 5. They are in good agreement with earlier studies (Hangala 1987, Höllta 1986, Schellekens 1980, Wever 1986). The estimates obtained by Hölttä (1986) and Schellekens (1980) are also shown in Fig. 5 to allow comparison. Garnet-cordierite temperatures of Schellekens, who used the thermometer of Currie (1971), were recalculated with the thermometer of Perchuk & Lavrent'eva (1983).

An indication of the $P_{H_2O}$ for the granulite domain can be obtained from the temperature and pressure estimates. The coexistence of garnet and cordierite related to the reaction: garnet + sillimanite + quartz = cordierite (Holdaway & Lee 1977) combined with $X_{Mg}$ values between 0.5 and 0.7 results in a maximum estimate for $P_{H_2O}$ of 0.4 $P_{tot}$. Similar estimates were obtained with the reaction: phlogopite + quartz = enstatite + K-feldspar + $H_2O$, using the equilibrium limits of Hansen et al. (1984). The $P_{H_2O}$ for the stable mineral paragenesis hypersthene-biotite-quartz-K-feldspar is estimated to lie between 0.2 and 0.4 $P_{H_2O}$ at temperatures of 750 ± 50° C and pressures of 4.8 ± 1 kbar.

At this stage it is emphasized that the prograde transition from amphibolite to granulite facies is essentially isobaric, with the highest observed temperatures in the core of the granulite domain where also the majority of the charnockitic rocks occur.

### *P-T path*

The results obtained through calculations of P-T diagrams using GEO-CALC allow a reconstruction of the P-T path for the Turku granulite area (Fig. 6). The prograde path can be detected from 610° C and 4.3 kbar, but little is known of previous P-T conditions. The absence of kyanite and the presence of andalusite in amphibolite facies rocks in the Svecofennian Schist Belt suggest that P-T conditions stayed below the kyanite field. From 610° C they progressed towards peak temperatures of 820° C at 5 kbar through near-isobaric heating, probably preceded by emplacement of intrusions. After peak metamorphic conditions were reached, pressures decreased at moderately decreasing tem-

*Table 6.* Mineral data for GEO-CALC

| Sample no. | Garnet | | | | Plagioclase | | | Orthopyroxene | | | Biotite | | | |
|---|---|---|---|---|---|---|---|---|---|---|---|---|---|---|
| | $X_{Gr}$ | $X_{Py}$ | $X_{Alm}$ | $X_{Sp}$ | $X_{An}$ | $X_{Ab}$ | $X_{Or}$ | $X_{Mg}$ | $X_{M1}$ | $X_{M2}$ | $X_{Mg}$ | $X_{Fe}$ | $X_K$ | $X_{OH}$ |
| Pelitic gneisses | | | | | | | | | | | | | | |
| CN143p | 0.02 | 0.20 | 0.76 | 0.02 | 0.24 | 0.74 | 0.02 | | | | 0.53 | 0.36 | 0.98 | 0.75 |
| CN143m | 0.03 | 0.21 | 0.74 | 0.02 | 0.25 | 0.73 | 0.02 | | | | 0.43 | 0.45 | 0.99 | 0.79 |
| CN143r | 0.03 | 0.17 | 0.78 | 0.02 | 0.20 | 0.79 | 0.01 | | | | 0.44 | 0.44 | 0.98 | 0.80 |
| HW166 | 0.03 | 0.25 | 0.71 | 0.03 | 0.26 | 0.72 | 0.01 | | | | 0.45 | 0.41 | 0.99 | 0.90 |
| CN083m | 0.03 | 0.21 | 0.74 | 0.02 | 0.24 | 0.75 | 0.01 | | | | 0.38 | 0.48 | 0.98 | 0.93 |
| CN083r | 0.03 | 0.13 | 0.81 | 0.03 | 0.21 | 0.78 | 0.01 | | | | 0.39 | 0.48 | 0.98 | 0.94 |
| CN139m | 0.03 | 0.19 | 0.76 | 0.03 | 0.27 | 0.72 | 0.01 | | | | 0.39 | 0.47 | 0.98 | 0.90 |
| CN139r | 0.03 | 0.15 | 0.79 | 0.04 | 0.25 | 0.73 | 0.02 | | | | 0.41 | 0.46 | 0.97 | 0.88 |
| Gt-Opx bearing metavolcanic rocks | | | | | | | | | | | | | | |
| HW041m | 0.13 | 0.15 | 0.69 | 0.03 | 0.78 | 0.22 | 0.00 | 0.37 | 0.04 | 0.03 | 0.37 | 0.56 | 0.99 | 0.94 |
| HW041r | 0.14 | 0.13 | 0.70 | 0.03 | 0.78 | 0.22 | 0.00 | 0.41 | 0.04 | 0.03 | 0.37 | 0.56 | 0.99 | 0.94 |
| HW137m | 0.09 | 0.13 | 0.74 | 0.03 | 0.41 | 0.58 | 0.01 | 0.35 | 0.02 | 0.04 | 0.37 | 0.53 | 0.99 | 1.00 |
| HW138m | 0.06 | 0.16 | 0.74 | 0.04 | 0.38 | 0.62 | 0.01 | 0.44 | 0.04 | 0.03 | 0.46 | 0.48 | 0.99 | 0.94 |

Column 1: m = matrix; r = rim; p = prograde. Orthopyroxene: $X_{Mg} = Mg/(Mg + Fe^{2+})$; $X_{M1} = X_{Al\text{-}VI} + X_{Ti} + X_{Fe\text{-}III}$; $X_{M2} = X_{Ca} + X_{Mn} + X_{Na}$; Biotite: $X_{Mg}$ ($X_{Fe}$) = Mg(Fe)/(Mg + Fe + Ti + $Al^{VI}$ + Mn).

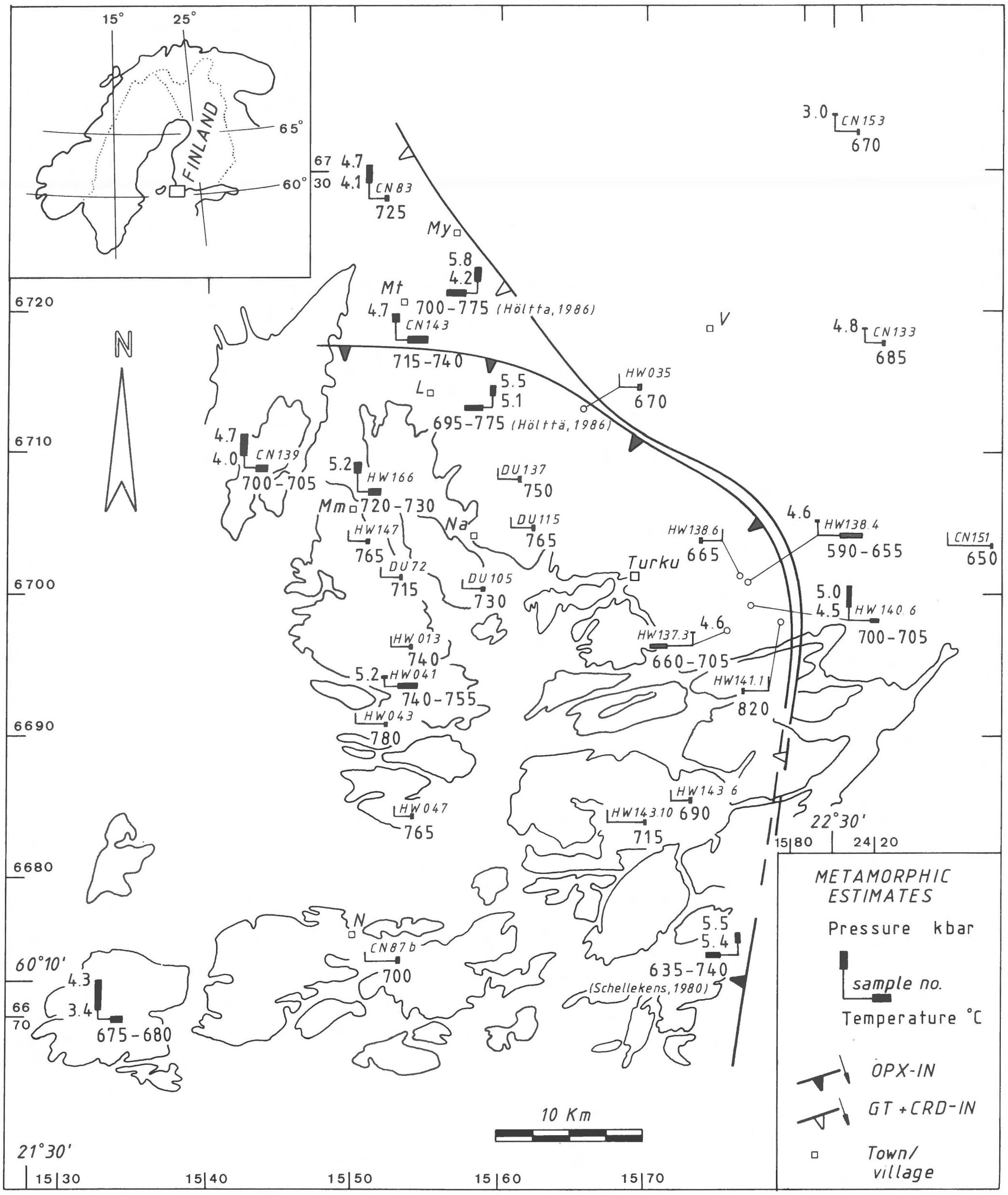

*Fig. 5.* Regional distribution of temperatures and pressures obtained through geothermobarometric methods presented in italics in Tables 5a–c. P-T estimates of Hölttä (1986) and Schellekens (1980; recalculated values *see text*) are shown for comparison.

peratures, which results in a clockwise P-T path. We infer that this part of the P-T path reflects cooling during uplift and concomitant erosion or tectonic denudation.

The cooling trajectory of the clockwise P-T path shows a remarkable difference with the P-T cooling path for the West Uusimaa granulite Complex presented by Hartel (1988) and Touret & Hartel (1990) (Fig. 6). Their retrograde path corresponds to one of near-isobaric or isochoric cooling till approximately 450–500° C, followed by fast uplift. Bohlen (1987) has proposed that this type of cooling path, often resulting in an anti-clockwise P-T path, is the

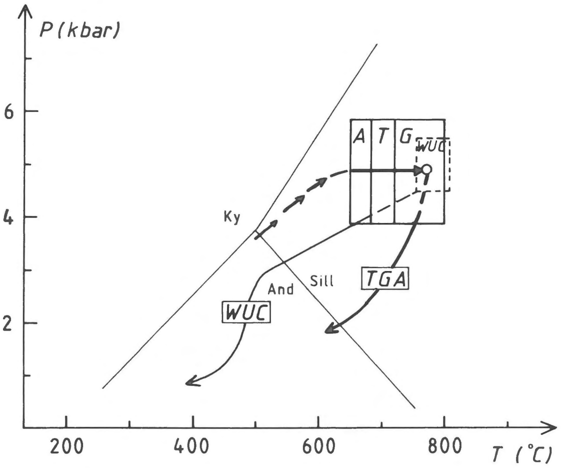

*Fig. 6.* P-T boxes for the three domains in the Turku granulite area (TGA): A = Amphibolite domain, T = Transition zone, and G = Granulite domain. Al-silicate stability fields according to Holdaway (1971). The P-T loop is mainly based on values obtained with the GEO-CALC software package (see also Figs 4A, B). Also shown are peak P-T conditions and retrograde P-T evolution of the West Uusimaa granulite Complex (WUC) (Touret & Hartel 1990).

general rule for regionally exposed granulite facies terrains.

## *LP-Granulite domains in the Svecofennian Schist Belt*

Despite differences in the retrograde P-T path, the Turku granulite area presents many similarities with the two other granulite domains occurring in the Svecofennian Schist Belt, the West Uusimaa granulite Complex and the Sulkava area:

(1) The P-T estimates for the West Uusimaa granulite Complex are 700–825° C, 3–5 kbar, and $P_{H_2O} \leq 0.35\,P_{tot}$. For the Sulkava area estimates are 740–765° C and 4.2–4.4 kbar with $p_{H_2O} = 0.2\,P_{tot}$. These estimates are comparable to those of the Turku area and also belong to the low-pressure type.

(2) The three granulite domains show an apparently prograde transition from amphibolite to granulite facies metamorphism.

(3) The estimated ages for the three granulite domains are between 1850 and 1800 Ma.

On the basis of these similarities, we assume that the granulite facies metamorphism in all three areas in the Svecofennian Schist Belt occurred during the same thermal event at a late stage of the orogeny. The late Svecofennian granitoids, whose occurrence is limited to this belt, may be closely related to this thermal event. These granitoids crystallized at 650° C and intruded just after peak metamorphic conditions (Hölttä 1986).

Although the granulite domains were presumably formed during the same event, they differ in a number of respects:

As stated before, the cooling trajectories are significantly different for the West Uusimaa granulite Complex and the Turku granulite area. Furthermore, the influence of external fluids differs considerably. In the West Uusimaa granulite Complex, granulite facies metamorphism was accompanied by a large influx of $CO_2$-rich fluids (Schreurs 1985a, Schreurs & Westra 1986). Quartz in orthopyroxene-bearing mobilizates and quartz in the host rocks are filled with high-density $CO_2$-rich fluid inclusions.

A fluid inclusion study in the Turku granulite area yields no conclusive evidence for the presence of large quantities of high-density $CO_2$-rich inclusions (Van Duin 1992). No indication has been found for a high influx of $CO_2$-rich fluids accompanying the granulite facies metamorphism. This does not necessarily imply that $CO_2$-rich fluids were never involved: the regional post-metamorphic evolution in the Turku granulite area, i.e. decompression at high temperatures, will generate drastic overpressures in any syn-metamorphic fluid inclusion, which necessarily leads to its transposition and disappearance (Touret 1989). Therefore, even if fluids were present, there was little chance to become preserved in fluid inclusions.

In the Turku area the granulite facies metamorphism is closely related to the occurrence of charnockitic plutonic rocks. These plutonic rocks show a complete sequence from gabbro to charno-enderbite, which has not been described in the other areas. These plutonic rocks yield U/Pb zircon ages of 1850–1840 Ma (Van Duin 1992) and they have been described as intra-orogenic intrusions significantly different from most early Svecofennian granitoids (Suominen 1991). The age of the charnockitic rocks in the Turku area broadly coincides with the assumed age of regional metamorphism. This coincidence of low-pressure granulite metamorphism and the intrusion of a melt, as possible heat source, has been postulated or proved to exist for many granulite terrains (Frost & Frost 1987).

## *Implications for a thermotectonic model*

The occurrence of low-pressure type granulite domains imposes severe restrictions on any postulated thermotectonic model, especially in a belt which has formerly been described as being the result of continent-arc collision and crustal thickening (Gaál 1982, Korsman et al. 1984, etc.).

In the Ladoga–Botnian Bay Zone, a clear correlation is observed between the occurrences of granulite facies metamorphism and deep-seated fracturing (Gaál 1986). Large-scale, deep-seated faulting has not yet been observed in the Svecofennian Schist Belt.

According to Thompson (1989) the type of assumed prograde P-T path described for the Turku area, which is similar to the West Uusimaa granulite Complex, is typical for crustal thickening. Thompson proposes an elegant model for the origin of granitic magmatism and regional metamorphism in low-P-high-T terrains through moderate overthickening of thinned sialic crust.

With crustal thickening, low-pressure amphibolite facies conditions are easily attained. An additional heat supply must be involved to account for the local temperature increase which characterizes the granulite domain. In the Turku granulite area, the metamorphism seems closely related to the occurrence of charnockitic rocks, whereas in the West Uusimaa granulite Complex the metamorphism is related to a $CO_2$-rich fluid. The two local phenomena associated with granulite facies metamorphism might be different aspects of an identical process, operating close to the base of the crust and possibly responsible for the granulite metamorphism. Loosveld & Etheridge (1990) proposed a model in which crustal thickening may lead to (convective) thinning of the mantle lithosphere and, subsequently, to upwelling of hot asthenospheric mantle. Asthenospheric temperatures close to the base of the crust may lead to melting of the lithospheric mantle, and emplacement of magma at the base of the crust. Subsequent generation of melt in the lower crust and intrusion of these magmas at higher levels of the crust may account for the transport of heat (and fluids) (Frost & Frost 1987, Frost et al. 1990). The presence of an intrusion-related thermal anomaly, which seems to characterize the prograde granulite transition in the Turku granulite area, has also been observed in other areas (Barber & Yardley 1985). However, metamorphic overprinting observed in several charnockitic sills close to the boundary of the granulite domain suggests that here granulite facies metamorphism succeeded the intrusion of the charnockite suite and was therefore not caused by its intrusion. Above, we described the intrusion of the charnockite suite as the ultimate result of asthenospheric temperatures close to the base of the crust. This thermal anomaly might not only be responsible for the generation of magmas (Turku) and release of fluids (West Uusimaa), but also for granulite metamorphism at mid-crustal levels. Nevertheless, intrusion-related granulite facies metamorphism may still be valid for the core of the granulite domain where the majority of the charnockitic rocks are found and where the highest temperatures are recorded.

Bohlen (1987) likewise advocates intrusion of magmas beneath or into a given terrain to account for granulite facies conditions in a continental arc environment, especially in paired amphibolite-granulite terrains. Emplacement of large quantities of magma at the base of the crust will provoke simultaneous heating and tectonic loading through crustal thickening, thus resulting in an anti-clockwise P-T path. When, subsequently, the rate of magmatic intrusion decreases, isostatic restoration leads to decompression at more or less constant temperature (clockwise P-T evolution). The remarkable differences between the West Uusimaa granulite Complex and the Turku granulite area might simply be due to relatively small variations in the importance of underplating versus uplift rate during and immediately after peak metamorphic conditions.

## Acknowledgements

The authors are grateful to Professor J.L.R. Touret for his enthusiasm and positive criticism with which he guided us through the first drafts of this paper. Our appreciation goes to Dr. L. Westra, who introduced us to the area and who organized this research project. We also thank Dr. P. Maaskant for reviewing an early version of the manuscript. Dr. R.L.M. Vissers and an anonymous referee are gratefully acknowledged for their critical remarks which improved the quality of this paper significantly. This study forms part of the Ph.D study of J.A. van Duin performed at the Vrije Universiteit, Amsterdam. The research of C.P. Nieman, incorporated in this paper, benefitted from a grant financed by the Schürmann Foundation (research grant no. 1987/07). Electronprobe microanalyses were performed at the electronmicroprobe laboratory of the Institute of Earth Sciences, Vrije Universiteit, with financial support by W.A.C.O.M. (Research Group of Analytical Chemistry of Minerals and Rocks) subsidized by the Netherlands Organization for Scientific Research (NWO).

## References

Aranovich, L.Y. & K.K. Podlesskii 1983 The cordierite-garnet-sillimanite-quartz equilibrium: experiments and applications – In: Adv. Phys. Geoch. 3: 173–198

Barber, J.P. & B.W.D. Yardley 1985 Conditions of high grade metamorphism in the Dalradian of Connemara, Ireland – J. Geol. Soc. London 142: 87–96

Berman, R.G. 1988 Internally consistent thermodynamic data for minerals in the system $Na_2O$-$K_2O$-CaO-MgO-FeO-$Fe_2O_3$-$AL_2O_3$-$SiO_2$-$TIO_2$-$H_2O$-$CO_2$ – J. Petrol. 29: 445–522

Berman, R.G. T.H. Brown & E.H. Perkins 1987 GEO-CALC: Software for calculation and display of pressure-temperature-composition phase diagrams – Am. Mineral. 72: 861–862

Bohlen, S.R. 1987 Pressure-temperature-time paths and a tectonic model for the evolution of granulites – J. Geology 95: 617–632

Bohlen, S.R. & E.J. Essene 1979 A critical evaluation of two-pyroxene thermometry in Adirondack granulites – Lithos 12: 335–345

Brown, T.H., R.G. Berman & E.H. Perkins 1987 GEO-CALC: A software package for rapid calculation of stable pressure-temperature-composition phase diagrams – Geol. Soc. Amer. 1987 Annual meeting (Abs.) 19–7: 603

Brown, T.H., R.G. Berman & E.H. Perkins 1988 GEO-CALC: Software package for calculation and display of pressure-temperature-composition phase diagrams using an IBM or compatible personal computer – Computers & Geosciences 14-3: 279–289

Currie, K.L. 1971 The reaction: 3 cordierite = 2 garnet + 4 sillimanite + 5 quartz, as a geological thermometer in the Opinicon Lake Region, Ontario – Contrib. Mineral. Petrol. 33: 215–226

Edelman, N. & M. Jaanus-Järkälä 1984 A plate tectonic interpretation of the Precambrian of the Archipelago of southwestern Finland – Geol. Surv. Finland, Bull. 325: 33 pp

Ehlers, C. & A. Lindroos 1986 Stratigraphy and geochemistry in the Proterozoic mafic volcanic rocks of the Nagu-Korpo area. SW-Finland – Prec. Res. 32: 297–315

Essene, E.J. 1982 Geological thermometry and barometry – In: J.M. Ferry (ed.): Characterisation of Metamorphism through Mineral Equilibria. Reviews in Mineralogy 10: 153–206

Ferry, J.M. & F.S. Spear 1978. Experimental calibration of the paritioning of Fe and Mg between biotite and garnet – Contrib. Mineral. Petrol. 66: 113–117

Front, K. & P.A. Nurmi 1987 Characteristics and Geological Setting of Synkinematic Svecokarelian Granitoids in Southern Finland – Prec. Res. 35: 207–224

Frost, B.R. & C.D. Frost 1987 $CO_2$, melts and granulite metamorphism – Nature 327: 503–506

Frost, B.R., C.D. Frost & J.L.R. Touret 1990 Magmas as a source of heat and fluids in granulite metamorphism – In: D. Bridgewater (ed.): Fluid Movements – Element Transport and the Composition of the Deep Crust: 1–18

Gaál, G. 1982 Proterozoic tectonic evolution and late Svecokarelian plate deformation of the Central Baltic Shield – Geol. Rundschau 71: 158–170

Gaál, G. 1986 2200 million years of crustal evolution: the Baltic Shield – Bull. Geol. Soc. Finland 58: 149–168

Ghent, E.D. 1976 Plagioclase-garnet-$Al_2SiO_5$-quartz: A potential geobarometer-geothermometer – Am. Mineral. 61: 710–714

Ghent, E.D. & M.Z. Stout 1981 Geobarometry and geothermometry of plagioclase-biotite-garnetmuscovite assemblages – Contrib. Mineral. Petrol. 76: 92–97

Grant, J.A. & P.W. Wiebelen 1971 Retrograde zoning in garnet near the second sillimanite isograd – Am. J. Sci. 270: 281–296

Hackman, V. 1923 Der Pyroxen-granodiorite von Kakskerta bei Åbo und seine Modifikationen – Bull. Comm. Géol. Finlande 61

Hangala, L.S. 1987 The early Proterozoic Zn-Pb-Cu massive sulfide deposit at Attu, SW Finland – Geol. Surv. Finland, Bull. No. 341

Hansen, E.C., R.C. Newton & A.S. Janardhan 1984 Fluid inclusions in rocks from the amphibolite-facies gneiss to charnockite progression in southern Karnataka, India: Direct evidence concerning the fluids of granulite metamorphism – J. Metam. Geol. 2: 249–264

Harley, S. 1984 An experimental study of the partitioning of Fe and Mg between garnet and orthopyroxene – Contrib. Mineral. Petrol. 86: 359–373

Härme, M. 1960 The general geologic map in Finland, Turku, Sheet B1, scale 1:400,000

Härme, M. 1965 On potassium migmatites of southern Finland – Bull. comm. Géol. Finlande, 219: 43 pp

Hartel, T.H.D. 1988 The cooling history of metapelites from the West Uusima Complex, southwest Finland – Int. Report, Vrije Universiteit, Amsterdam

Hietanen, A. 1947 Archean geology of the Turku district in southwestern Finland – Bull. Geol. Soc. Am. 58: 1019–1084

Holdaway, M.J. 1971 Stability of andalusite and the aluminium silicate phase diagram – Am. J. Sci. 271: 97–131

Holdaway, M.J. & S.M. Lee 1977 Fe-Mg Cordierite stability in high-grade pelitic rocks based on experimental, theoretical and natural observations – Contrib. Mineral. Petrol 63: 175–198

Hölttä, P. 1986 Observations on the metamorphic reactions and PT conditions in the Turku granulite area – Geol. Surv. Finland, Bull. No. 339: 43–58

Huhma, H. 1986 Sm-Nd, U-Pb and Pb-Pb Isotopic Evidence for the Origin of Early Proterozoic Svecokarelian Crust in Finland – Geol. Surv. Finland, Bull. No. 337

Indares, A. & J. Martignole 1985 Biotite-garnet thermometry in granulite facies, the influence of Ti and Al in biotite – Am. Mineral. 70: 272–278

Kays, M.A. 1976 Comparative geochemistry of migmatized, interlayered quartzofeldspathic and pelitic gneisses: a contribution form rocks of southern Finland and northeastern Saskatchewan – Prec. Res. 3: 433–462

Korsman, K. 1977 Progressive metamorphism of the metapelites in the Rantasalmi Sulkava area, southeast Finland – Geol. Surv. Finland, Bull. No. 290

Korsman, K., P. Hölttä, T. Hautala & P. Wasenius 1984 Metamorphism as an indicator of evolution and structure of the crust in eastern Finland – Geol. Surv. Finland, Bull. No. 328

Kretz, R. 1982 Transfer and exchange equilibria in a portion of the pyroxene quadrilateral as deduced from natural and experimental data – Geoch. Cosmoch. Acta 46: 411–421

Lindsey, D.H. 1983 Pyroxene thermometry – Am. Mineral. 68: 477–493

Loosveld, R.J.H. & M. A. Etheridge 1990 A model for low-pressure facies metamorphism during crustal thickening – J. Metam. Geol. 8: 257–267

Mori, T. & D.H. Green 1978 Laboratory duplication of phase equilibria observed in natural garnet lherzolites – J. Geol. 86: 83–97

Nabelek, P.I., D.H. Lindsley & S.R. Bohlen 1987 Experimental examination of two-pyroxene graphical thermometers using natural pyroxenes with application to metaigneous pyroxenes from the Adirondack Mountains, New York – Contrib. Mineral. Petrol. 97: 66–71

Newton, R.C. & B.J. Wood 1979 Thermodynamics of water in cordierite and some petrologic consequences of cordierite as a hydrous phase – Contrib. Mineral. Petrol. 68: 391–405

Newton, R.C. & H.T. Haselton 1981 Thermodynamics of the garnet-plagioclase-$Al_2SiO_5$-quartz barometer. In: R.C. Newton, A. Navrotsky & B.J. Wood (eds.): Thermodynamics of Minerals and Melts. Advances in Physical Geochemistry – Vol. 1, Springer, Berlin 131–148

Newton, R.C. & D. Perkins-III 1982 Thermodynamic calibration of geobarometers based on the assemblages garnet-plagioclase-orthopyroxene-(clinopyroxene)-quartz – Am. Min. 67: 203–222

Patchett, P.J. & O. Kouvo 1986 Origin of continental crust of 1.9–1.7 Ga age: Nd isotopes and U-Pb zircon ages in the Svecokarelian terrain of South Finland – Contrib. Mineral. Petrol. 92: 1–12

Perchuk, L.L. 1986 The course of metamorphism – Int. Geol. Rev. 28: 1377–1400

Perchuk, L.L. & L.Y. Aranovich 1986 Improvement of the biotite-garnet geothermometer: correction for the fluorine content of biotite – Scripta Technica: 130–133

Perchuk, L.L. & I.V. Lavrent'eva 1983 Experimental Investigation of exchange equilibria in the system cordierite-garnet-biotite In: S.K. Saxena (ed.): Kinetics and Equilibrium in Mineral Reactions. Advances in Physical Geochemistry – Vol. 3, Springer, Berlin, 199–239 pp

Perkins, D.III & S.J. Chipera 1985 Garnet-orthopyroxene-plagioclase-quartz barometry: refinement and application to the English River subprovince and the Minnesota River valley – Contrib. Mineral. Petrol. 89: 69–80

Perkins, D.III, E.J. Essene & L.A. Marcotty 1982 Thermometry and barometry of some amphibolite-granulite facies rocks from the Otter Lake area, southern Quebec – Canadian J. Earth Sci. 19: 1759–1774

Perkins, E.H., T.H. Brown & R.G. Berman 1986 PT-system, TX-system, PX-system: three programs for calculation of pressure-temperature-composition phase diagrams – Comp. Geosci. 12: 749–755

Ploegsma, M. 1989 Shear zones in the West Uusimaa Area, SW Finland – Unpubl. Ph. D. thesis, Vrije Universiteit, Amsterdam, 134 pp

Schellekens, J.H. 1980 Application of the garnet-cordierite geothermometer and geobarometer to gneisses of Attu SW Finland: an indication of P and T conditions of the lower granulite facies – N. Jb. Miner. Mh. 1: 11–19

Schreurs, J. 1985a The West Uusimaa low pressure thermal dome, SW Finland – Ph.D. Thesis, Vrije Universiteit, Amsterdam, 179 pp

Schreurs, J. 1985b Prograde metamorphism of metapelites, garnet-biotite thermometry and prograde changes of biotite chemistry in high-grade rocks of West Uusimaa, southwest Finland – Lithos 18: 69–80

Schreurs, J. & L. Westra 1986 The thermotectonic evolution of a Proterozoic, low pressure, granulite dome, West Uusimaa, SW Finland – Contrib. Mineral. Petrol 93: 236–250

Sen, S.K. & A. Bhattacharya 1984 An orthopyroxene-garnet thermometer and its application to the Madras charnockites – Contrib. Mineral. Petrol. 88: 64–71

Simonen, A. 1980 The Precambrium in Finland – Geol. Surv. Finland Bull. 304: 1–58

Suominen, V. 1991 The chronostratigraphy of southwestern Finland with special reference to Postjotnian and Subjotnian diabases – Geol. Surv. Finland Bull. 356: 100 pp

Thompson, A.B. 1976 Mineral reactions in pelitic rocks II. Calculation of some P-T-X(FeMg) phase relations – Am. J. Sci. 276: 425–454

Thompson, P.H. 1989 Moderate overthickening of thinned sialic crust and the origin of granitic magmatism and regional metamorphism in low-P-high-T terranes – Geology 17: 520–523

Touret, J.L.R. 1989 Fluid control in the lower crust – Niedersachsische Ak. Geowissenschaften, Heft 1 (Gesteinfluide): 57–68

Touret, J.L.R. & T.H.D. Hartel 1990 Synmetamorphic fluid inclusions in granulites – In: D. Vielzeuf & Ph. Vidal (eds.): Granulites and Crustal Evolution. NATO Advanced Science Institutes Series C: Mathematical and Physical Sciences – Vol. 311: 397–418

Tracy, J.R., P. Robinson & A.B. Thompson 1976 Garnet composition and zoning in the determination of temperature and pressure of metamorphism, central Massachusetts – Am. Mineral. 61: 762–775

Vaasjoki, M. 1977 Rapakivi granites and other postorogenic rocks in Finland: the age and the lead isotopic composition of certain associated galena mineralization – Geol. Surv. Finland Bull. 294: 64 pp

Van Duin, J.A. 1987 High-grade metamorphic rocks of the West Uusimaa Complex: A low pressure thermal dome? – Int. Report, Vrije Universiteit, Amsterdam

Van Duin, J.A. 1992 The Turku granulite area, SW Finland: a fluid-absent Svecofennian granulite occurrence – Ph.D. Thesis, Vrije Universiteit, Amsterdam, 234 pp

Wells, P.R.A. 1977 Pyroxene thermometry in simple and complex systems – Contrib. Mineral. Petrol. 62: 129–139

Westra, L. & J. Schreurs 1985 The West Uusimaa Granulite Complex (Finland): an Early Proterozoic low pressure Thermal Dome. NATO Advanced Study Institute, Moi, Norway

Wever, H.E. 1986 Geothermometry and geobarometry of high grade metamorphic rocks from the Turku region, Southwest Finland – Int. Report, Vrije Universiteit, Amsterdam

Wood, B.J. 1974 The solubility of alumina in orthopyroxene ceoxisting with garnet – Contrib. Mineral. Petrol. 46: 1–15

Wood, B.J. & S. Banno 1973 Garnet-orthopyroxene and orthopyroxene —-clinopyroxene relationships in simple and complex system – Contrib. Mineral. Petrol. 42: 109–124